NASA/TM—2013–216320

VAB Sway Investigation

Robert C. Youngquist
NASA Kennedy Space Center

Curtis M. Ihlefeld
NASA Kennedy Space Center

Stephen M. Simmons
EASi, Engineering Services Contract, Kennedy Space Center

John E. Lane
EASi, Engineering Services Contract, Kennedy Space Center

Stanley O. Starr
NASA Kennedy Space Center

January 2013

NASA/TM—2013–216320

VAB Sway Investigation

Robert C. Youngquist
NASA Kennedy Space Center

Curtis M. Ihlefeld
NASA Kennedy Space Center

Stephen M. Simmons
EASi, Engineering Services Contract, Kennedy Space Center

John E. Lane
EASi, Engineering Services Contract, Kennedy Space Center

Stanley O. Starr
NASA Kennedy Space Center

National Aeronautics and
Space Administration

Kennedy Space Center

January 2013

The NASA STI Program Office ...in Profile

Since its founding, NASA has been dedicated to the advancement of aeronautics and space science. The NASA Scientific and Technical Information (STI) Program Office plays a key part in helping NASA maintain this important role.

The NASA STI Program Office is operated by Langley Research Center, the lead center for NASA's scientific and technical information. The NASA STI Program Office provides access to the NASA STI Database, the largest collection of aeronautical and space science STI in the world. The Program Office is also NASA's institutional mechanism for disseminating the results of its research and development activities. These results are published by NASA in the NASA STI Report Series, which includes the following report types:

- TECHNICAL PUBLICATION. Reports of completed research or a major significant phase of research that present the results of NASA programs and include extensive data or theoretical analysis. Includes compilations of significant scientific and technical data and information deemed to be of continuing reference value. NASA counterpart of peer-reviewed formal professional papers, but having less stringent limitations on manuscript length and extent of graphic presentations.

- TECHNICAL MEMORANDUM. Scientific and technical findings that are preliminary or of specialized interest, e.g., quick release reports, working papers, and bibliographies that contain minimal annotations. Does not contain extensive analysis.

- CONTRACTOR REPORT. Scientific and technical findings by NASA-sponsored contractors and grantees.

- CONFERENCE PUBLICATION. Collected papers from scientific and technical conferences, symposia, seminars, or other meetings sponsored or co-sponsored by NASA.

- SPECIAL PUBLICATIONS. Scientific, technical, or historical information from NASA programs, projects, and missions, often concerned with subjects having substantial public interest.

- TECHNICAL TRANSLATION. English-language translations of foreign scientific and technical material pertinent to NASA's mission.

Specialized services to complement the STI Program Office's diverse offerings include creating custom thesauri, building customized databases, organizing and publishing research results...even providing videos.

For more information about the NASA STI Program Office, see the following:

- Access the NASA STI Program Home Page at http://www.sti.nasa.gov

- E-mail your question via the internet to help@sti.nasa.gov

- Fax your question to the NASA STI Help Desk at (301) 621-0134

- Phone the NASA STI Help Desk at (301) 621-0390

- Write to:
  NASA STI Help Desk
  NASA Center for Aerospace Information
  1721 Standard Drive
  Hanover, MD 21076-1320

Acknowledgments

The research team gratefully acknowledges the contributions made by the following individuals:

a. Bobby Williams, VAB Operations Leader, Dept. 93510, United Space Alliance

b. James Bolton, VAB Operations Manager, NASA KSC, GP-O2-B

c. Jeffrey Brink, AST Tech Engineer Ops Mgmt, NASA KSC, LX-D1

d. Robert Cox, Engineering Designer, QinetiQ North America

e. Edward Muktarian, PE, System Engineering & Integration, SGT Inc.

Available from:

NASA Center for AeroSpace Information (CASI)
7121 Standard Drive
Hanover, MD 21076-1320
(301) 621-0390

National Technical Information Service (NTIS)
5285 Port Royal Road
Springfield, VA 22161-2171
(703) 605-6000

This report is also available in electronic form at URL http://www.sti.nasa.gov/ and http://ntrs.nasa.gov/search.jsp.

Contents

Figures

Tables

This page intentionally left blank.

ABBREVIATIONS AND ACRONYMS

KSC	John F. Kennedy Space Center
LED	light-emitting diode
UTC	Coordinated Universal Time
SODAR	sonic detection and radar
VAB	Vehicle Assembly Building

This page intentionally left blank.

ABSTRACT

The Vehicle Assembly Building (VAB) was constructed in the mid-1960s to house the Saturn V moon rocket while it was being assembled. Designed to withstand hurricanes and tropical storms, the VAB has a foundation consisting of 30,000 cubic yards of concrete strengthened by 4,225 steel rods driven 160 feet into limestone bedrock. The goal of the VAB Sway Investigation, which began collecting data in April 2010 and ended in November 2012, was to quantify the displacement or *sway* of the VAB as a function of wind loading. Unlike other tall buildings whose height is much greater than their average cross-section dimension, the VAB is roughly a box with a height L = 526 ft. In the case of skyscrapers, building sway is characterized by a damped oscillation that may be on the order of 0.1 Hz to 0.5 Hz. The VAB, on the other hand, is an over-damped harmonic oscillator characterized by a simple displacement in the direction of the wind load. This conclusion is based on the fact that no oscillatory behavior was ever observed in the entire VAB sway data set. Even though the investigation and data collection continued for over 2 years, the wind speeds observed during that time did not exceed 50 kts. Therefore, the final data analysis consists of an extrapolation formula, which expresses the magnitude of the displacement d as a function of wind speed v [kts], height above the ground h [ft], and number of standard deviations n above the mean:

$$d(n,v,h) = \alpha\, e^{bn\sigma}(hv/L)^2 \quad \text{[in]} \quad , \tag{1}$$

where $\alpha = 0.0001591$ [in·kts^{-2}], $b \equiv \sqrt{5}\,\ln 10 = 5.1487$ [in^{-1}], and $\sigma = 0.092$ [in], are determined from the data analysis. Table 1 is an evaluation of Equation (1) for various wind speeds and for n = 0, 1 , and 2. The meaning of confidence level is discussed in the Discussion and Summary section.

Table 1. Equation (1) Evaluated for Various Confidence Levels *C* at *h* = 300 ft

v [kts] (10-min peak)	0·σ (C = 50%)	1·σ (C = 84%)	2·σ (C = 98%)
10	0.005	0.008	0.013
20	0.021	0.033	0.054
30	0.047	0.075	0.12
40	0.083	0.13	0.21
50	0.13	0.21	0.34
60	0.19	0.30	0.48
70	0.25	0.41	0.66
80	0.33	0.53	0.82
90	0.42	0.67	1.1
100	0.52	0.83	1.3
110	0.63	1.0	1.6
120	0.74	1.2	1.9

This page intentionally left blank.

VAB SWAY INVESTIGATION

1 BACKGROUND

The Vehicle Assembly Building (originally named the *Vertical* Assembly Building) was used to assemble American manned launch vehicles from 1968 through 2011. Completed in 1966, the VAB was originally built to allow for the vertical assembly of the Saturn V rocket for the Apollo program. It was then used for housing Space Shuttle external fuel tanks and flight hardware, and was where Space Shuttle orbiters were mated with their solid rocket boosters and external fuel tanks. The VAB is 526 feet (160.3 m) tall, 716 feet (218.2 m) long, and 518 feet (157.9 m) wide. It covers 8 acres and encloses 129,428,000 cubic feet (3,665,000 m^3) of space. Entry to the bays inside the building is made through the four largest doors in the world. Each door is 456 feet (139.0 m) high and takes 45 minutes to completely open or close. Another large door on the north entry that leads to the transfer aisle was widened by 40 feet (12.2 m) to accommodate the Shuttle orbiter. A slot was added at the center of this north entry to allow for passage of the orbiter's vertical stabilizer.

It is well known that buildings sway in response to wind, as well as to earthquakes, and the taller the structure, the more they can sway. Because Kennedy Space Center (KSC) is occasionally assaulted by tropical or hurricane force winds, data on the VAB's sway, collected from instrumentation positioned as indicated in Figure 1, is essential to help characterize the VAB facilities so that they can be used by commercial customers in the future.

Figure 1. Locations for Data Collection

Data from the nearest wind towers (http://trmm.ksc.nasa.gov/) is used to correlate wind velocity and direction to position data from the telescope.

2 TEST PROCEDURE

The data acquisition strategy for this study was implemented with a Meade RCX400 telescope, positioned on the VAB floor in High Bay 4 as shown in Figure 2, along with a target fixed to the ceiling (see Figure 3). The position of the target is recorded once per second with a computer (also shown in Figure 2) attached to a camera mounted at the end of the telescope. The telescope data is then compared to data from the wind towers in the vicinity of the VAB (Figure 1). Instrumentation is located on three elevations on the wind towers; data from the highest, at 54 ft, is used in this analysis. The primary goal of this project is to correlate the movement of the building as a result of wind only. Table 2 is a list of the 22 best-correlated data points extracted from telescope-target position data and the wind tower dataset.

Figure 2. Telescope Used for Data Collection

Meade RCX400 telescope pointed toward the ceiling in High Bay 4 with a PC running LabView image processing software.

Table 2. Correlation of Wind Data with VAB Displacement

(The correlation between wind data and VAB displacement is also shown as circles in Figure 6.)

Date	Wind speed (10-min peak)	Displacement *d* [in]	Average Wind Direction [deg]
10/27/2012	39	0.40	0
09/06/2012	30	0.12	260
09/09/2012	27	0.12	273
08/28/2012	32	0.08	226
08/27/2012	35	0.19	167
08/08/2012	34	0.21	0
07/22/2012	41	0.23	167
07/18/2012	32	0.15	250
06/25/2012-a	37	0.18	167
06/25/2012-b	38	0.23	250
06/06/2012	42	0.18	250
05/28/2012	40	0.18	178
04/06/2012	29	0.18	0
03/31/2012	44	0.54	300
03/04/2012	36	0.38	310
02/22/2012	26	0.27	330
09/14/2011	23	0.17	47
09/05/2011	31	0.13	250
08/28/2011	45	0.13	214
06/04/2010	31	0.09	226
05/17/2010	28	0.18	0
05/06/2010	35	0.13	250

Figure 3. Telescope Target

The telescope's target is mounted on the ceiling above the telescope in High Bay 4. As shown in the lower left, the target consists of three bright LEDs, in a rotated L-shaped pattern. The dimensions of the LED pattern are 1 inch × 3 inch.

3 DATA ANALYSIS

An example of correlated wind tower and telescope data is shown in the graph of Figure 4. At approximately 6 PM local time on August 8, 2012, a strong wind event occurred, lasting for well over an hour. The peak displacements (the differences between telescope and target positions) were only ¼ inch, but were very well correlated to the wind tower data. The peak wind, as shown in Figure 4, was only 35 kts, but the duration and broad impulsive character combined to generate a set of conditions that allowed the building position data to track the wind data. It is believed that a doubling of wind speed (70 kts in this case) will produce a quadrupling of the building sway, or 1 inch. This has not yet been confirmed, however; tropical force (70 kt) winds have not occurred since the hurricanes of 2004, or about 5 years before the deployment of the sway-tracking telescope.

In addition to wind-induced displacement, movement resulting from other sources, such as sun-induced heating and temperature cycling, as well as crane and heavy equipment operations, has been recorded. It is often difficult to distinguish the uncorrelated sources of telescope displacement noise, such as wind blowing through the large high bay doors. Since the telescope-target optical measurement reports a relative position, this measurement represents the maximum possible building sway, because it is statistically unlikely that the telescope and building would move in a way that would cancel out the real displacement. This sets a lower limit on displacement (but not an upper limit). In other words, the actual building displacement is equal to or less than the value measured by the displacement magnitude $(d_x^2 + d_y^2)^{1/2}$ in the raw data plots, such as that shown in Figure 4.

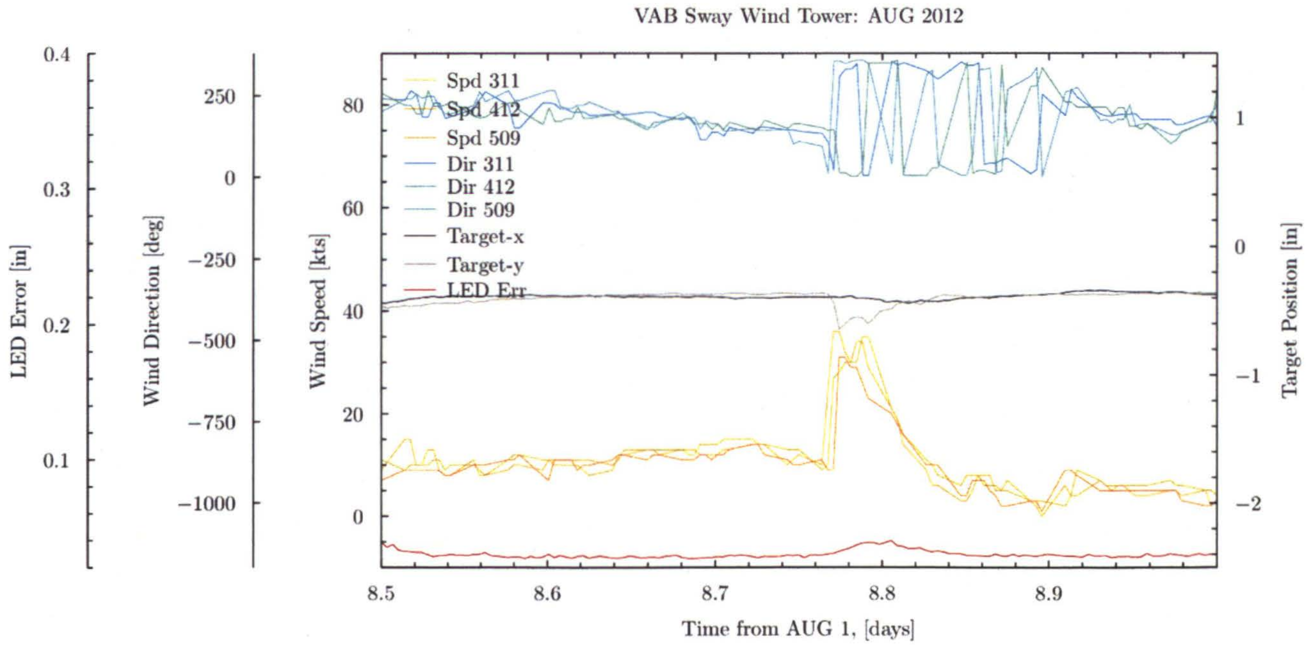

Figure 4. Data from August 8, 2012 Event

This wind event produced a well-correlated building displacement as measured by the telescope-target system. The wind direction was from the north, i.e., 0 degrees.

In most of the good correlations between VAB displacement and wind events, the wind events are short and usually associated with thunderstorms or other phenomena related to passing weather fronts. The August 28, 2011 data shown in Figure 5 is a prime example of a passing convective thunderstorm. When this occurs, it is common for the wind speed to increase dramatically, with an abrupt change in direction. (Directional change is usually characterized by a rotation of wind direction.) After the front (sometimes referred to a *gust front* or *outflow boundary*) passes, the wind speed and direction return to their previous *synoptic* state. The entire length of this event is on the order of one hour or less, with the peak wind state lasting only 10 to 15 minutes.

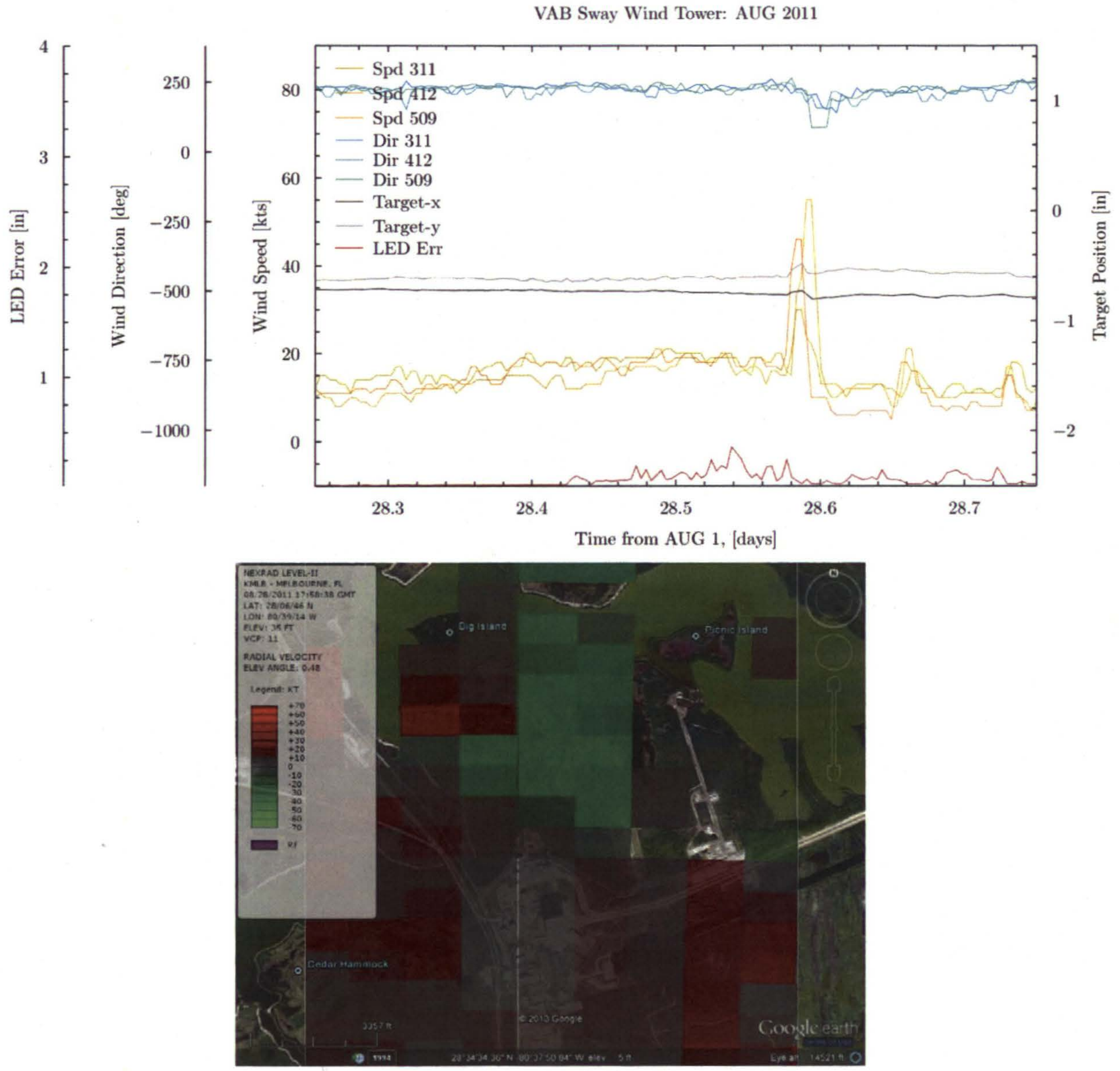

Figure 5. Example Thunderstorm Event and Associated Wind Direction Change over the VAB

The thunderstorm event occurred on August 28, 2011, 17:58 UTC. Note that the time scale on the plot corresponds to local time.

4 DISCUSSION AND SUMMARY

Figure 6 is a graph of Equation (1) as a function of wind speed for various values of n, and for h = 300 (green lines) and h = L (red lines). When the data (red circles) is viewed on a log-log plot, such as Figure 6, the scatter appears to be uniformly distributed about the mean (0-σ) line, shown as the bold red line. σ is calculated by first transforming the wind speed v and displacement building d to new variables $w = \log(v)$ and $u = \log(d)$. The transformed data $\{w, u(w)\}$ in the coordinate system is then rotated by $\theta = \tan^{-1} 2$, since the slope of the log-log plot is 2, corresponding to the initial model, which assumes that displacement is proportional to v^2. The displacement data in the rotated coordinate system can be modeled as a random variable x, which is approximately uniformly distributed about $x = 0$:

$$P(x) = \frac{1}{\sigma\sqrt{2\pi}} e^{-\frac{1}{2}\left(\frac{x}{\sigma}\right)^2} \quad , \tag{2}$$

where the standard deviation σ is computed in the standard way in this rotated coordinate system. In order to use σ in the original coordinate system of $\{v, d(v)\}$, an inverse rotation is performed followed by an anti-log transformation, arriving at:

$$d(n,v,h) = \alpha\, e^{bn\sigma} v^2 \quad [\text{in}] \quad , \tag{3}$$

where α and b are fit parameters. By multiplying Equation (3) by the height function, $(h/L)^2$, which accounts for the quadratic bending mode of the building, Equation (1) is obtained.

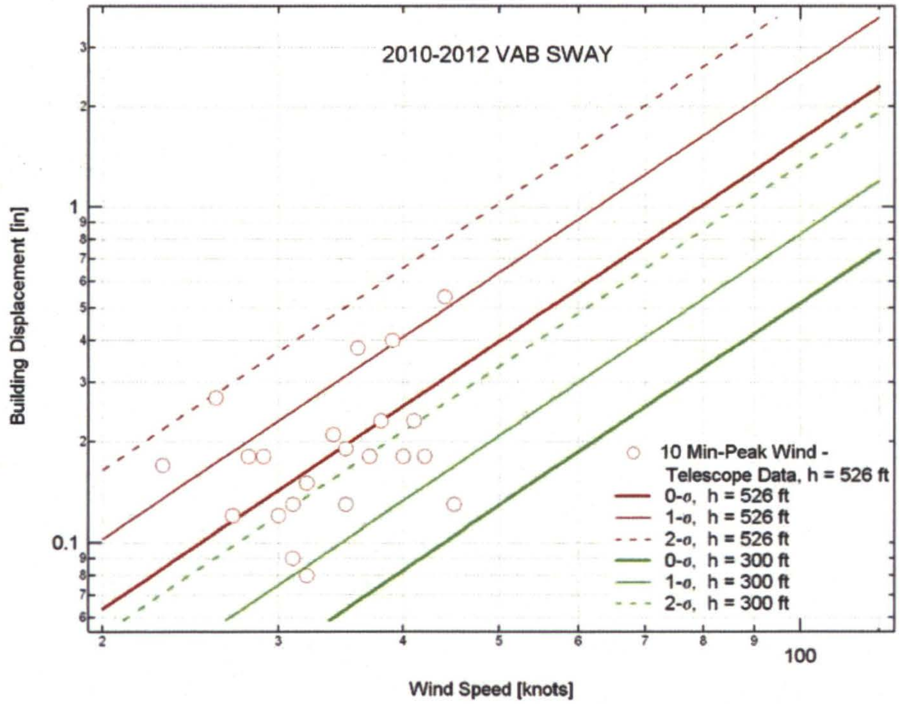

Figure 6. Building Displacement Correlated with Wind Speed

Figure 6 shows Equation (1) evaluated at the (red) top of the VAB ($h = L = 526$ ft) and (green) at $h = 300$ ft. The solid bold lines are the average response (C = 50% confidence level), the solid line is one standard deviation above the mean (C = 84% confidence level), and dotted lines are two standard deviations above the mean (C = 98% confidence level).

The confidence levels C in Table 1 are obtained by integrating Equation (2) from $-\infty$ to $n\sigma$:

$$C(n) = \int_{-\infty}^{n\sigma} P(x)dx$$
$$= \frac{1}{2}\left(1 + erf\left(\frac{n}{\sqrt{2}}\right)\right) \quad . \tag{4}$$

The confidence level C can then be interpreted in this context as the percent fraction of the distribution based on the telescope-target and wind tower data, such that a building displacement at a given confidence level (based on n) is less than or equal to d of Equation (1), corresponding to the fraction of $P(x)$ from $-\infty$ to $n\sigma$.

For this to have a more physical explanation, we need to discuss the error sources that contribute to the distribution and the measured standard deviation σ. The raw data can be decomposed into two main sources: (1) displacement that is correlated to the wind speed and direction at the tower, and (2) everything else. The second category corresponds to the sources mentioned in the previous section. The data used in this analysis (shown by circles in Figure 6) are only from the first category, i.e., where displacement is proportional to the wind speed and direction at the tower. For the purpose of this analysis, everything else was discarded. So the next question might be, What sources control the standard deviation σ, especially since all uncorrelated data was discarded? Many possibilities must be considered.

The first source that contributes to the probability distribution width is the likelihood that not all of the uncorrelated noise was removed from the data used in Figure 6. This is simply because the correlated portion of the displacement is riding on a background signal that is uncorrelated. So even though attempts have been made to remove that background noise, some of it will remain, or the attempt at removing (or filtering) leads to additional error.

However, we believe that the largest contribution of data scatter, quantified by σ (probability distribution width), can be investigated by answering the question, What is the actual wind speed acting on the VAB? Even though the wind towers are part of a quality-controlled weather data network for KSC and Cape Canaveral Air Force Station, they measure the wind at a specific point in space. Three wind towers were used for this analysis, as shown in Figure 1. The distance from the VAB to the towers is in a range from 2 km to 3 km. The wind tower measurement used in this analysis was taken at a height of 54 ft (the highest available sensor on the three towers used).

Another source of data scatter is the width of the time interval of the wind acting on the VAB. If the time interval is smaller than the response time of the building, the displacement will be smaller than the average trend. This could explain the circles under the main trend line (shown as the bold solid red line) in Figure 6. The circles above the line could be explained by wind forces at 300 ft that were greater than those measured by the wind towers at 54 ft. This is exemplified in the August 28, 2011 event shown in Figure 5, where the entire event lasted less than one hour and the peak winds were prevalent for less than 15 minutes. In this case, the building response time was longer than the wind event duration, and corresponds to a data point below the main trend line.

So the primary uncertainty is in determining actual wind speed across the surface of the VAB. Conceptually, this could be improved by wind towers at 0.5 km (not too close, else the building-induced wind circulation would perturb the measurement), and at a height of 300 ft. A SODAR wind measurement system near the VAB could, in theory, produce an ideal wind measurement dataset. On the other hand, the primary data source used to monitor wind speeds relevant to VAB operations should be the ones used to make the associated predictions of building displacement. If that primary source is wind towers near the VAB (within 2 km to 3 km), then the resulting data scatter shown in Figure 6 must be dealt with in an appropriate statistical manner for useful displacement predictions, as has been attempted in this report.

APPENDIX A. RAW DATA CORRESPONDING TO TABLE 2

The following 22 plots correspond to the entries of Table 2. Each plot contains wind speed and direction measured at the three towers shown in Figure 1. The horizontal and vertical target positions are also plotted, in black and grey. In order to extract a building sway direction, we need to approximate a local background position and apply it to the specific event. Flat lines in the telescope data usually indicate the crane blocking the telescope. The relative displacement of the building can then be converted into an angle for comparison with the wind direction recorded at the tower. Lastly, the LED error is plotted in red.

The target position is the average of the three LED positions, (x_0,y_0), (x_1,y_1), and (x_2,y_2) over a 5-minute period:

$$c_x = c_{x0} + \frac{1}{3N}\sum_{n=1}^{N}\left(x_0(n) + x_1(n) + x_1(n)\right) \tag{A-1}$$

$$c_y = c_{y0} + \frac{1}{3N}\sum_{n=1}^{N}\left(y_0(n) + y_1(n) + y_1(n)\right) \quad , \tag{A-2}$$

where c_{x0} and c_{y0} are constant offsets for the graph.

The LED error E (red line) is computed as the maximum of the 1 sec error over a 5-minute period, so that $N = 300$:

$$d_{01} = \left((x_0 - x_1)^2 + (y_0 - y_1)^2\right)^{1/2} \tag{A-3}$$

$$d_{12} = \left((x_1 - x_2)^2 + (y_1 - y_2)^2\right)^{1/2} \tag{A-4}$$

$$d_{20} = \left((x_2 - x_0)^2 + (y_2 - y_0)^2\right)^{1/2} \tag{A-5}$$

$$E = \left((d_{01} - 1)^2 + (d_{12} - 3)^2 + (d_{20} - 10^{1/2})^2\right)^{1/2} \quad , \tag{A-6}$$

where the LED separations are assumed to be 1, 3, and $10^{1/2}$ inch. A high error (under 0.5 inch) might indicate telescope movement, possibly from wind blowing past it from the high bay doors. An error higher than 0.5 inch usually indicates a missing LED (i.e., the camera does not detect it for a number of possible reasons). In some cases the error disappears from the plot for many days or weeks at a time. This occurs when the LabView imaging software fails to detect one or two LEDs. Fortunately, the measurement of the relative position of the target is not severely affected and useful building sway information can still be extracted.

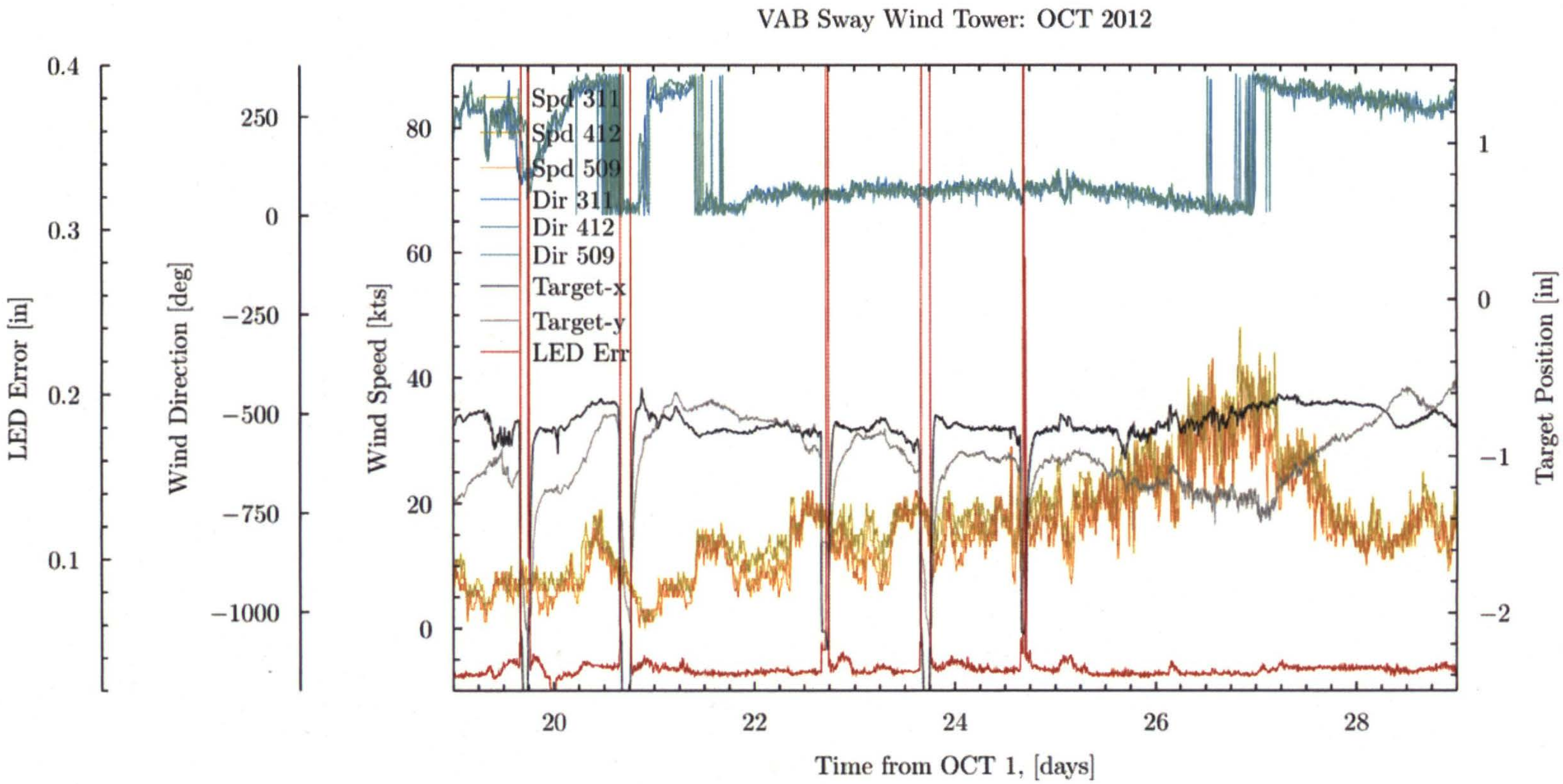
VAB Sway Wind Tower: OCT 2012
LED Error [in]
0.4
0.3
0.2
0.1
Wind Direction [deg]
250
0
−250
−500
−750
−1000
Wind Speed [kts]
80
60
40
20
0
Spd 311
Spd 412
Spd 509
Dir 311
Dir 412
Dir 509
Target-x
Target-y
LED Err
Target Position [in]
1
0
−1
−2
20
22
24
26
28
Time from OCT 1, [days]

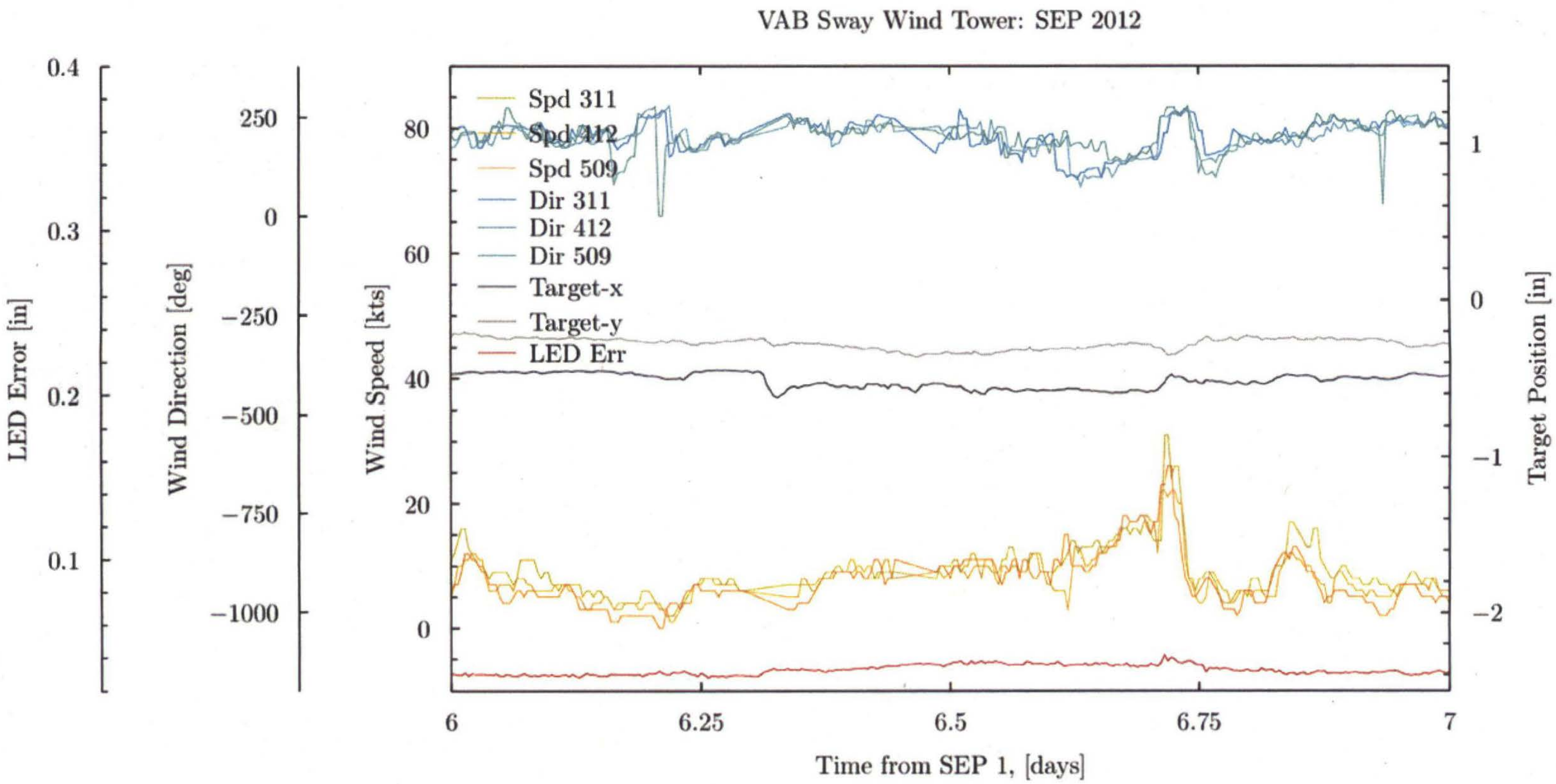
VAB Sway Wind Tower: SEP 2012
Spd 311
Spd 412
Spd 509
Dir 311
Dir 412
Dir 509
Target-x
Target-y
LED Err
LED Error [in]
Wind Direction [deg]
Wind Speed [kts]
Target Position [in]
Time from SEP 1, [days]

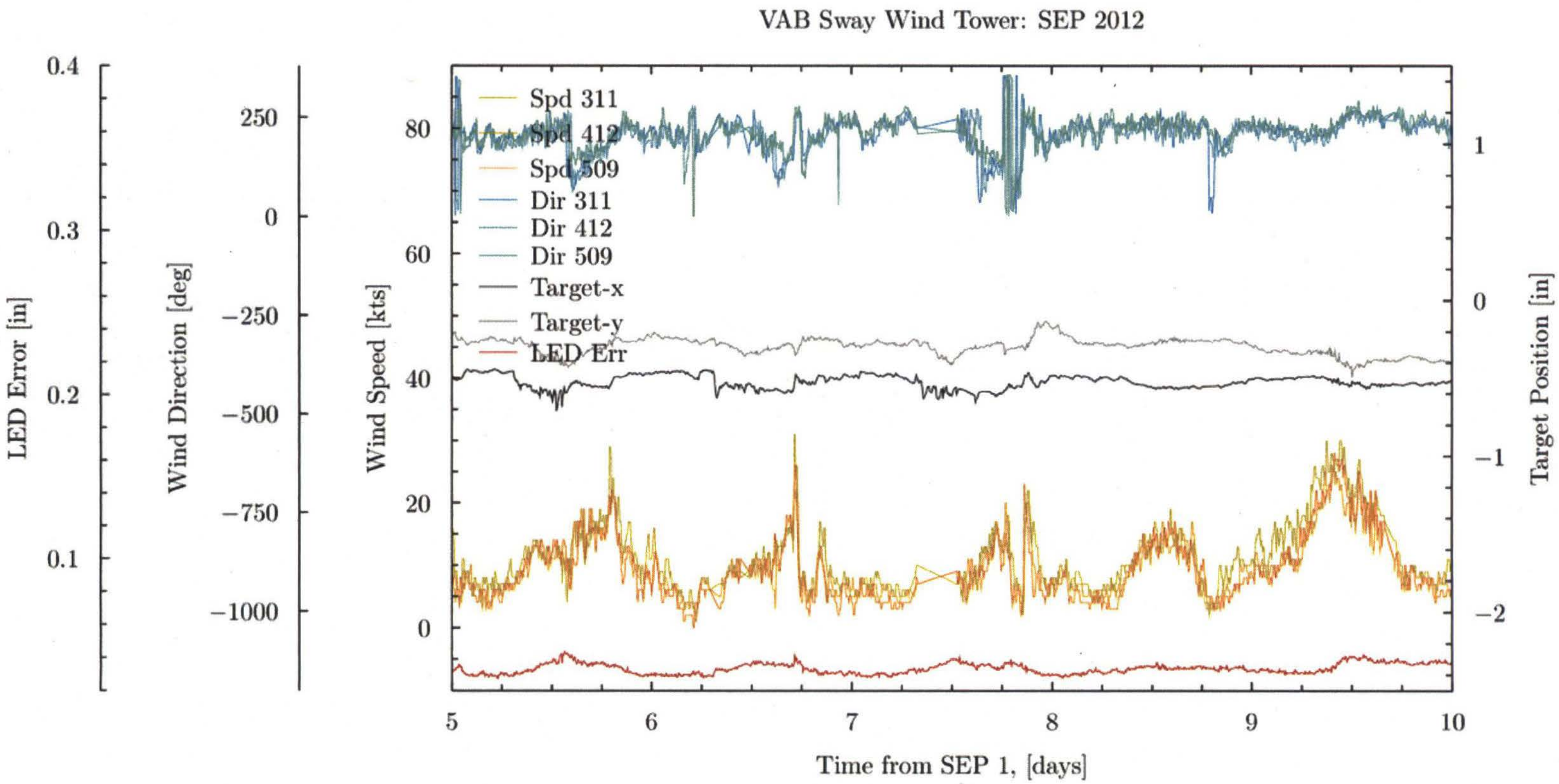
VAB Sway Wind Tower: SEP 2012
Spd 311
Spd 412
Spd 509
Dir 311
Dir 412
Dir 509
Target-x
Target-y
LED Err
LED Error [in]
Wind Direction [deg]
Wind Speed [kts]
Target Position [in]
Time from SEP 1, [days]

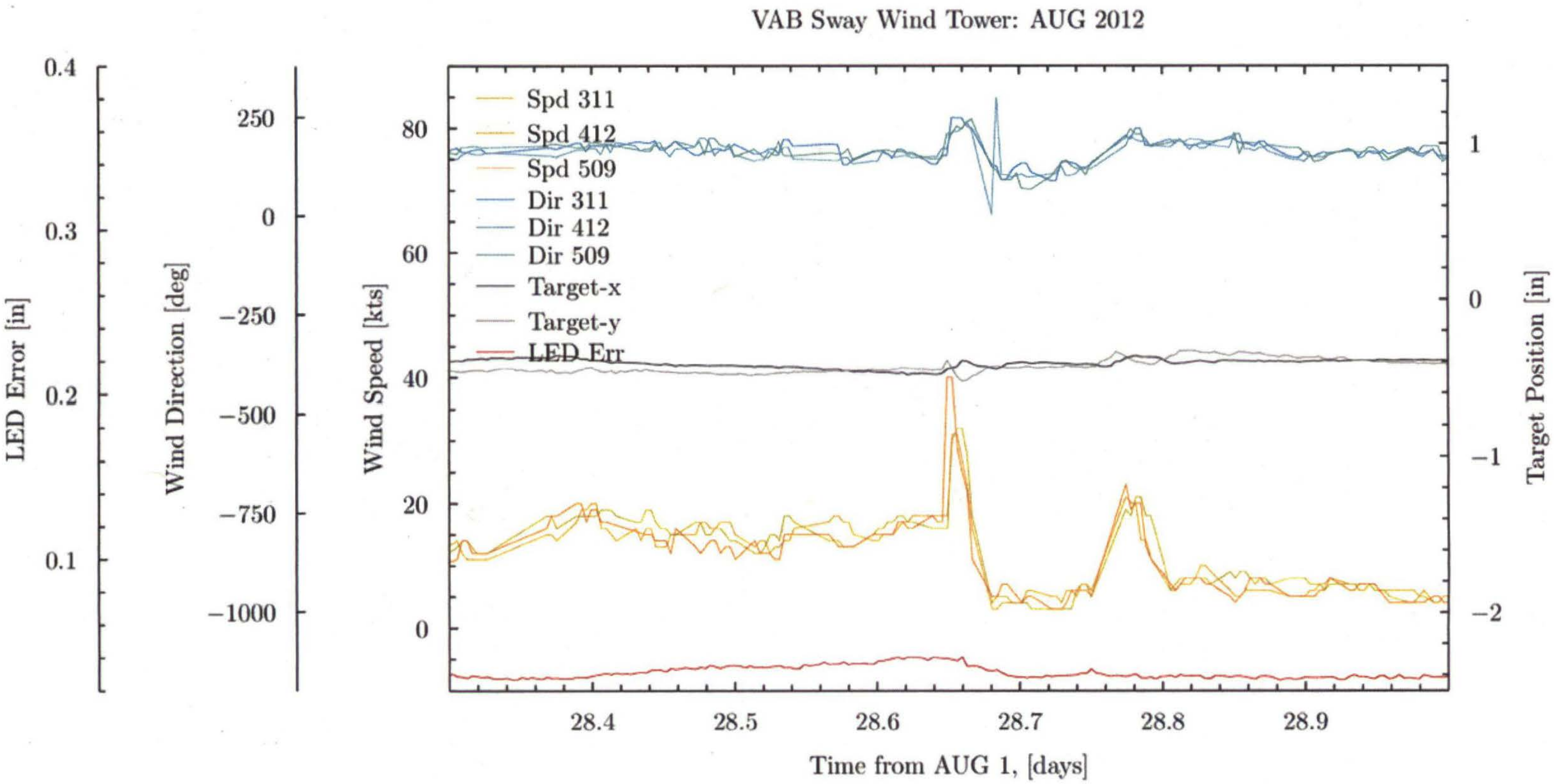
VAB Sway Wind Tower: AUG 2012
LED Error [in]
Wind Direction [deg]
Wind Speed [kts]
Target Position [in]
Time from AUG 1, [days]
Spd 311
Spd 412
Spd 509
Dir 311
Dir 412
Dir 509
Target-x
Target-y
LED Err

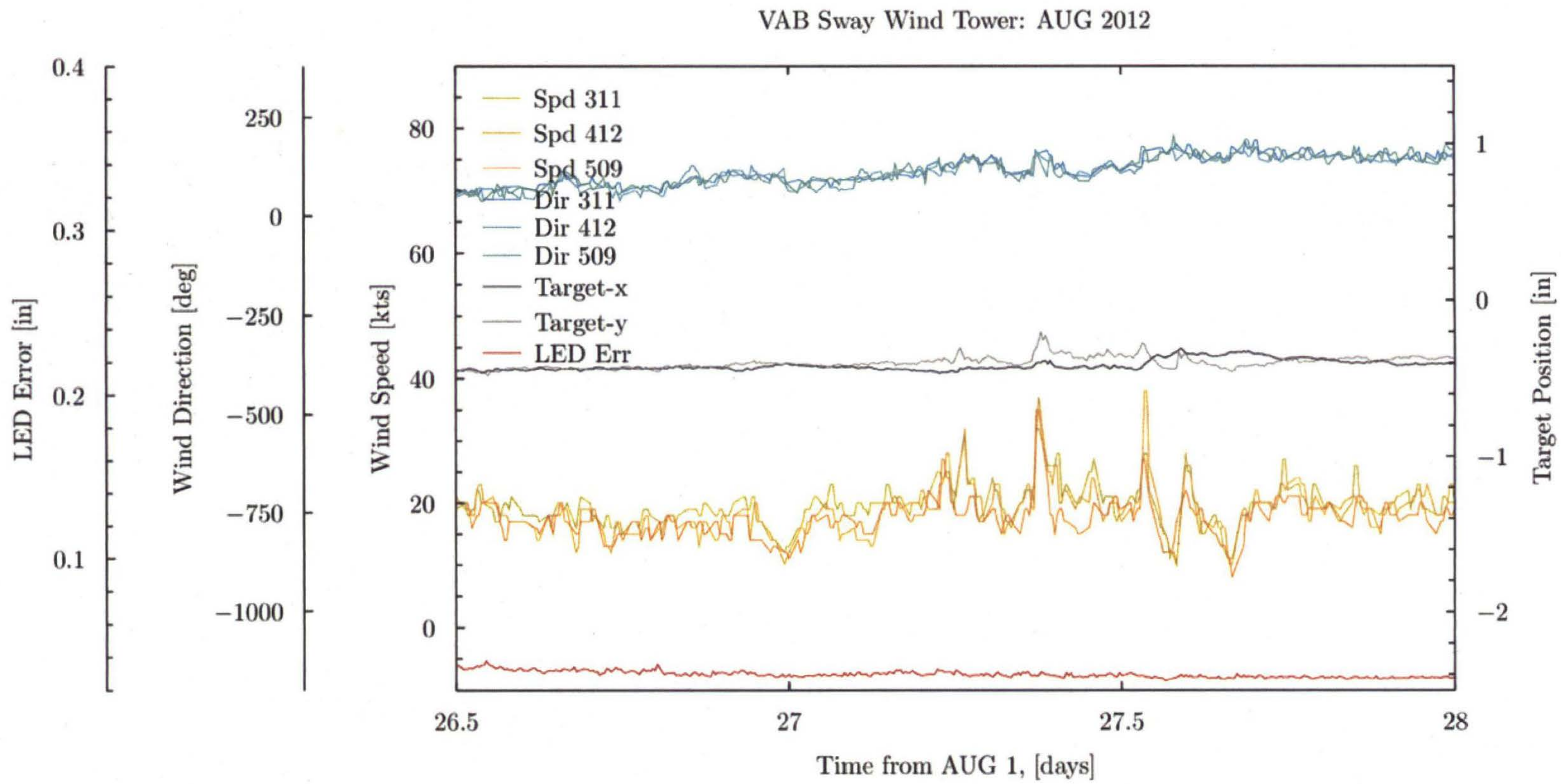
VAB Sway Wind Tower: AUG 2012
LED Error [in]
0.4
0.3
0.2
0.1
Wind Direction [deg]
250
0
−250
−500
−750
−1000
Wind Speed [kts]
80
60
40
20
0
Spd 311
Spd 412
Spd 509
Dir 311
Dir 412
Dir 509
Target-x
Target-y
LED Err
Target Position [in]
1
0
−1
−2
26.5
27
27.5
28
Time from AUG 1, [days]

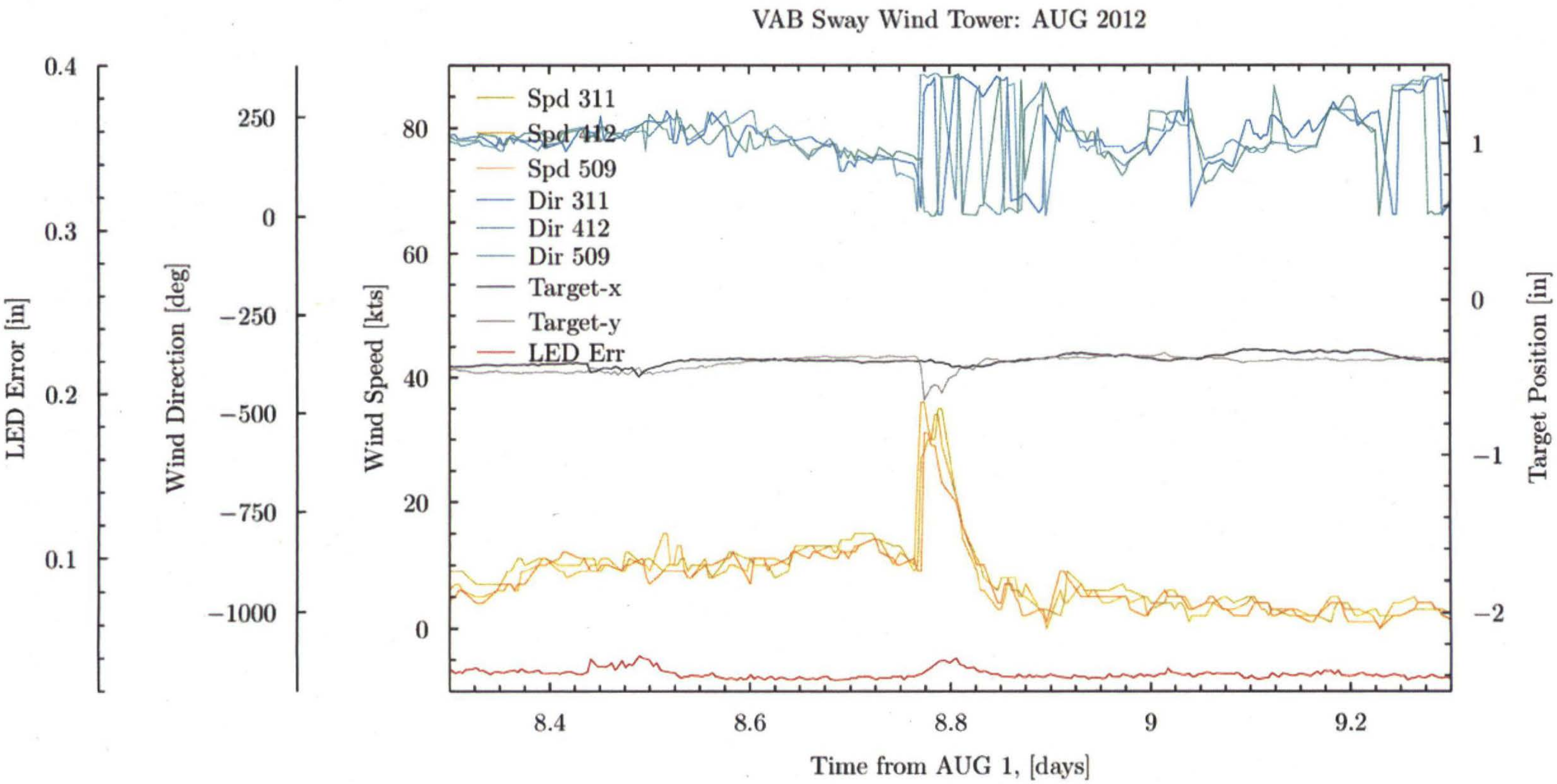
VAB Sway Wind Tower: AUG 2012
Spd 311
Spd 412
Spd 509
Dir 311
Dir 412
Dir 509
Target-x
Target-y
LED Err
LED Error [in]
Wind Direction [deg]
Wind Speed [kts]
Target Position [in]
Time from AUG 1, [days]
0.4
0.3
0.2
0.1
250
0
−250
−500
−750
−1000
80
60
40
20
0
1
0
−1
−2
8.4
8.6
8.8
9
9.2

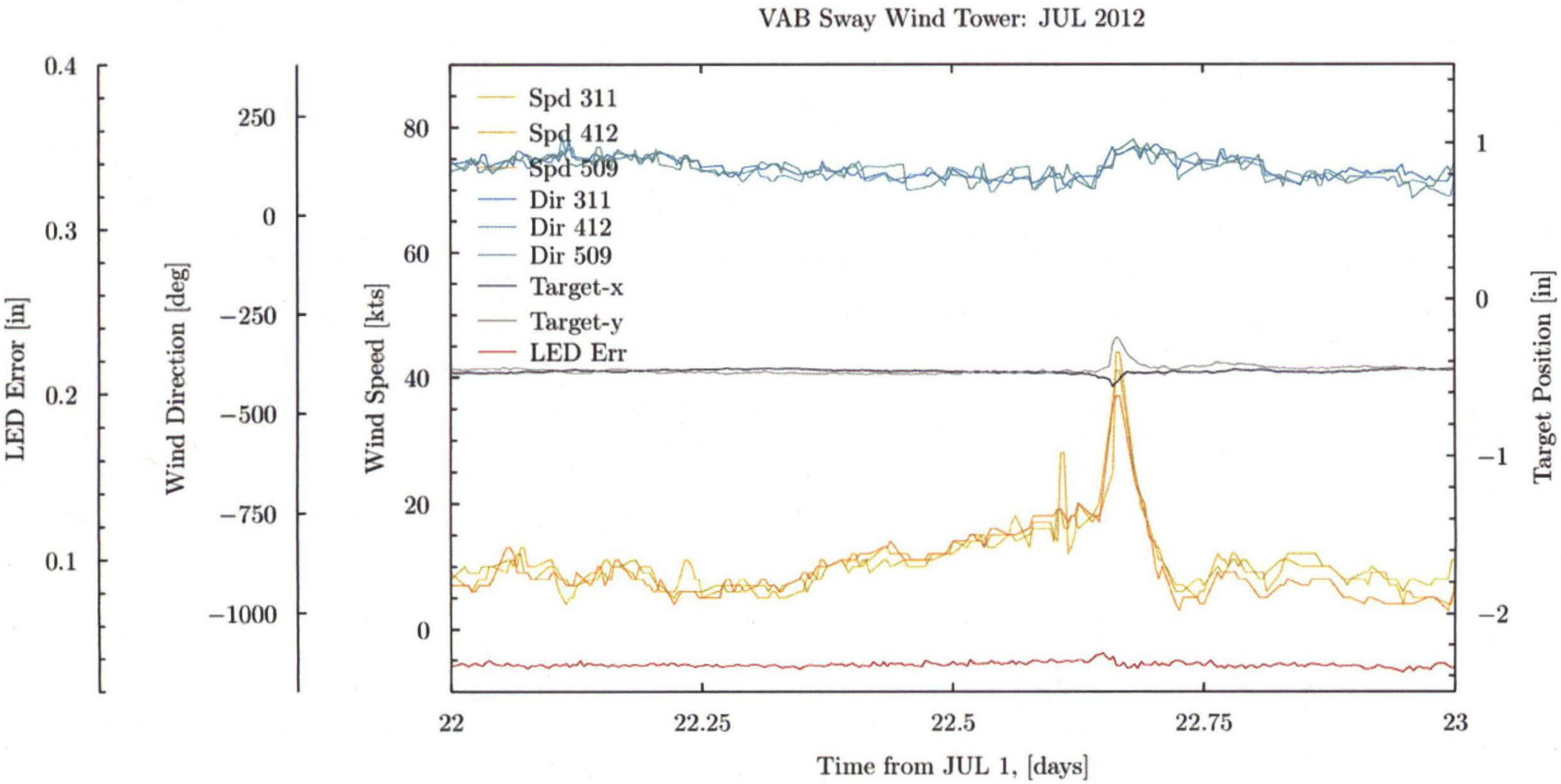
VAB Sway Wind Tower: JUL 2012
Spd 311
Spd 412
Spd 509
Dir 311
Dir 412
Dir 509
Target-x
Target-y
LED Err
LED Error [in]
Wind Direction [deg]
Wind Speed [kts]
Target Position [in]
Time from JUL 1, [days]
0.4
0.3
0.2
0.1
250
0
−250
−500
−750
−1000
80
60
40
20
0
1
0
−1
−2
22
22.25
22.5
22.75
23

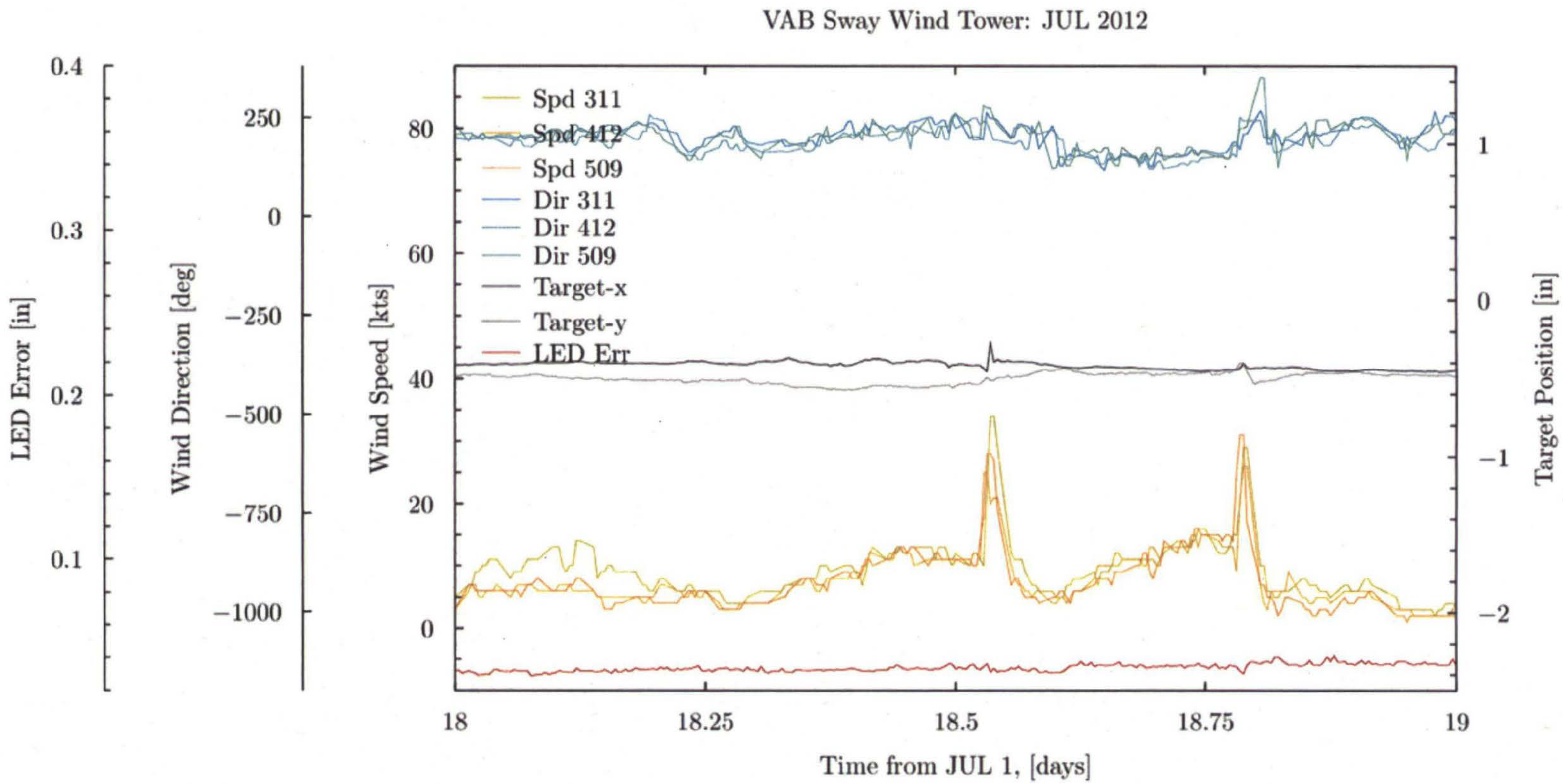
VAB Sway Wind Tower: JUL 2012
LED Error [in]
Wind Direction [deg]
Wind Speed [kts]
Target Position [in]
Time from JUL 1, [days]
Spd 311
Spd 412
Spd 509
Dir 311
Dir 412
Dir 509
Target-x
Target-y
LED Err
0.4
0.3
0.2
0.1
250
0
−250
−500
−750
−1000
80
60
40
20
0
1
0
−1
−2
18
18.25
18.5
18.75
19

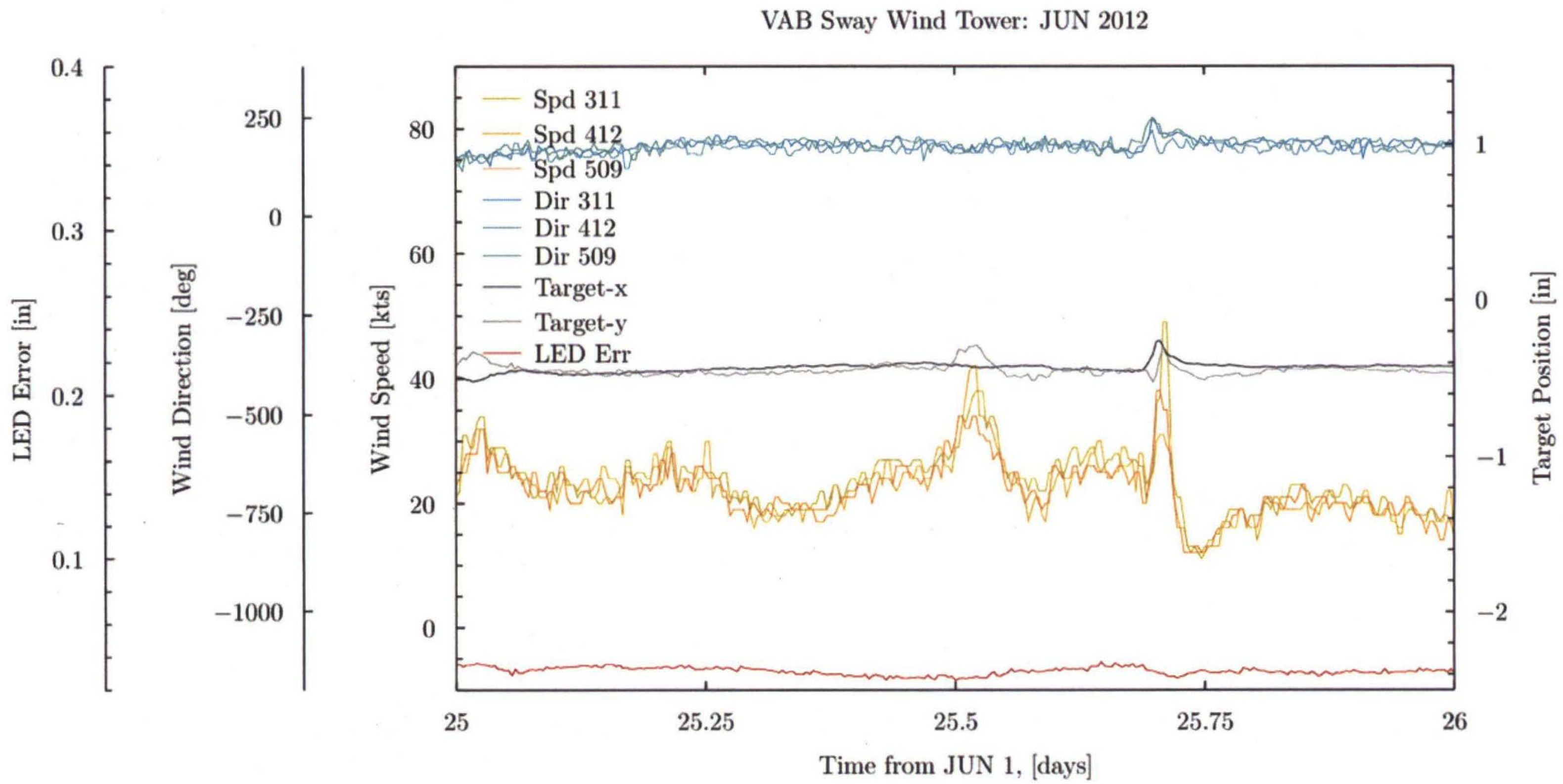
VAB Sway Wind Tower: JUN 2012
Spd 311
Spd 412
Spd 509
Dir 311
Dir 412
Dir 509
Target-x
Target-y
LED Err
LED Error [in]
Wind Direction [deg]
Wind Speed [kts]
Target Position [in]
Time from JUN 1, [days]
0.4
0.3
0.2
0.1
250
0
−250
−500
−750
−1000
80
60
40
20
0
1
0
−1
−2
25
25.25
25.5
25.75
26

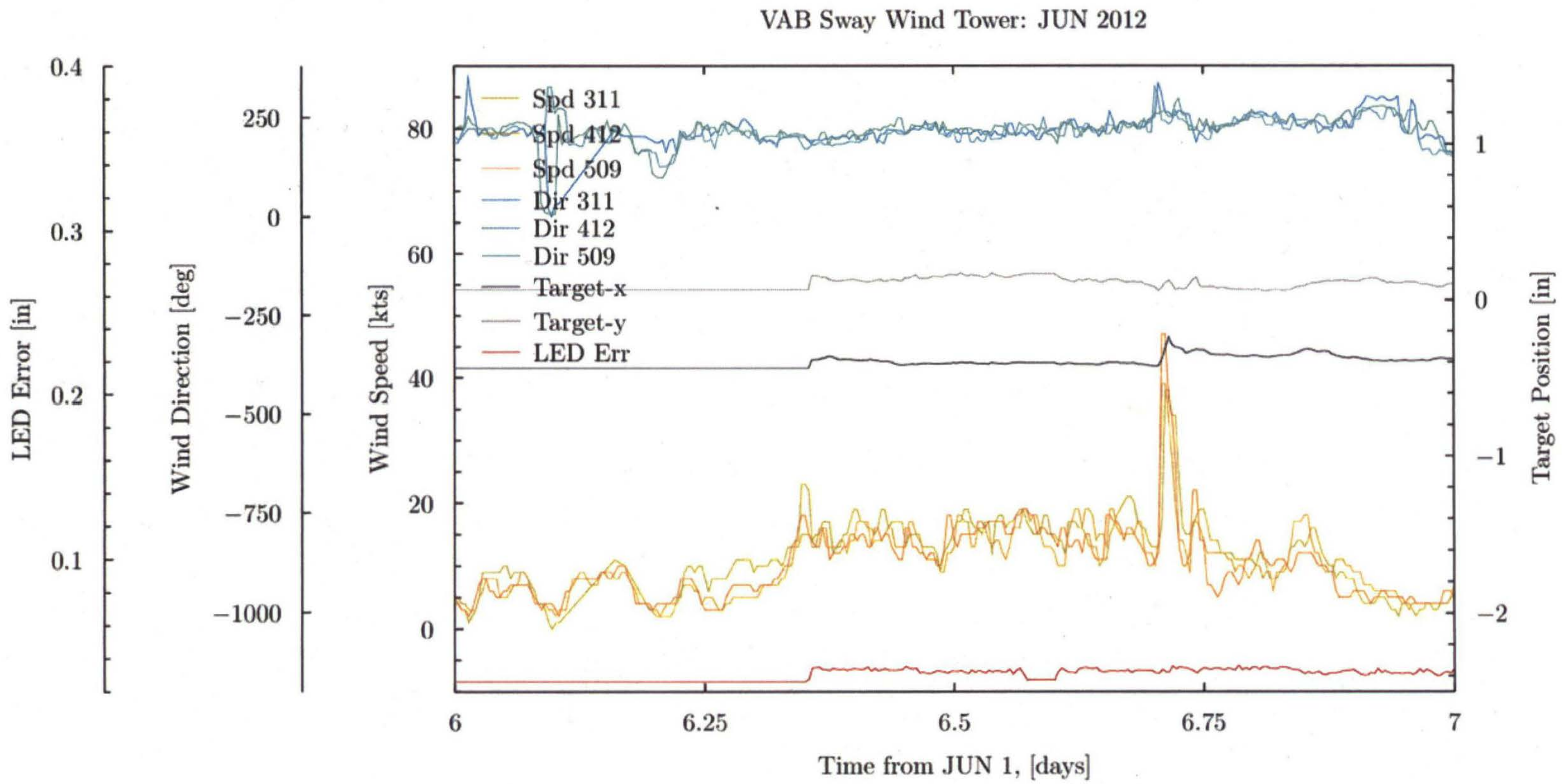
VAB Sway Wind Tower: JUN 2012
LED Error [in]
0.4
0.3
0.2
0.1
Wind Direction [deg]
250
0
−250
−500
−750
−1000
Wind Speed [kts]
80
60
40
20
0
Target Position [in]
1
0
−1
−2
Spd 311
Spd 412
Spd 509
Dir 311
Dir 412
Dir 509
Target-x
Target-y
LED Err
6
6.25
6.5
6.75
7
Time from JUN 1, [days]

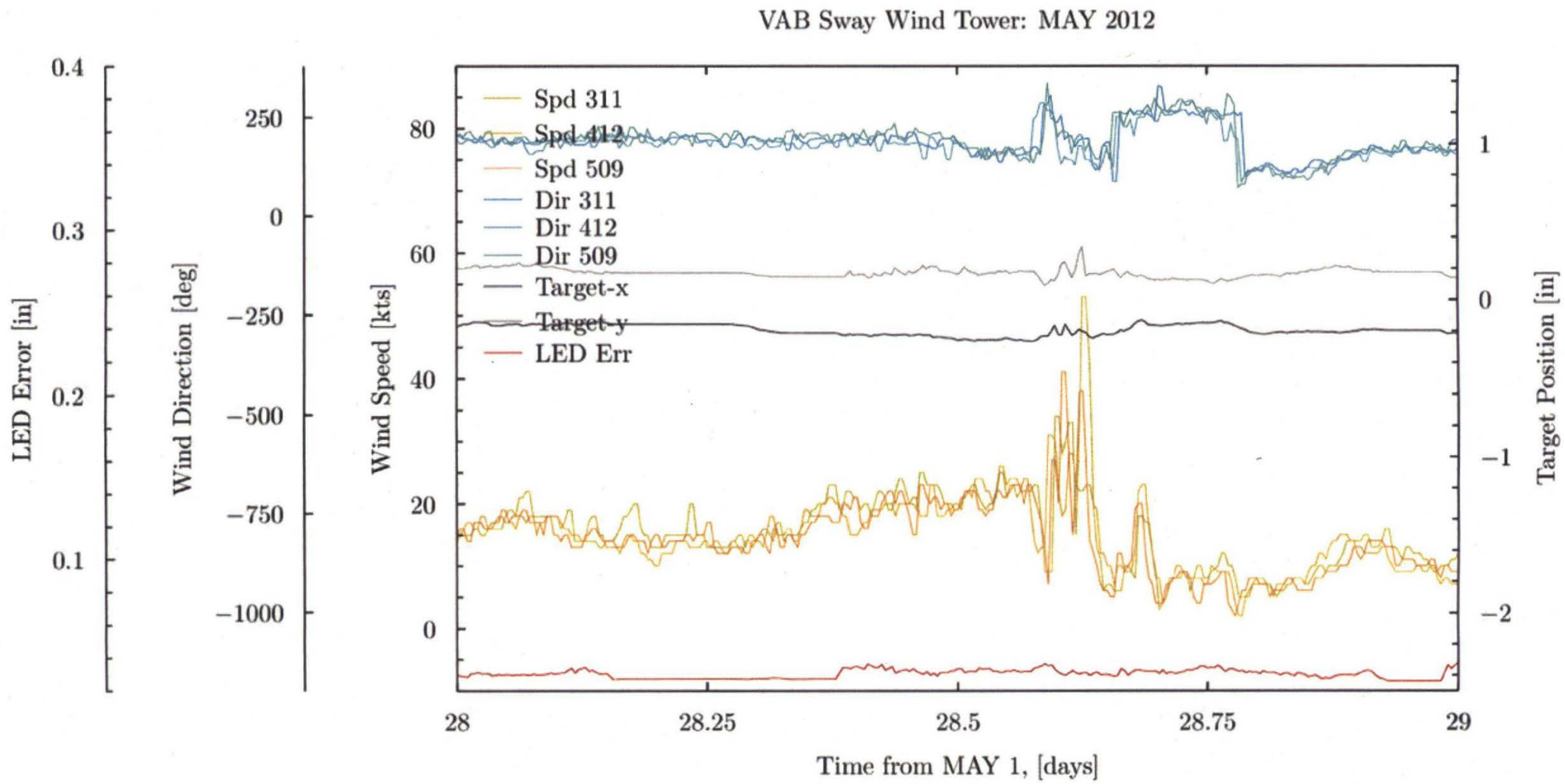
VAB Sway Wind Tower: MAY 2012
Spd 311
Spd 412
Spd 509
Dir 311
Dir 412
Dir 509
Target-x
Target-y
LED Err
LED Error [in]
0.4
0.3
0.2
0.1
Wind Direction [deg]
250
0
−250
−500
−750
−1000
Wind Speed [kts]
80
60
40
20
0
Target Position [in]
1
0
−1
−2
28
28.25
28.5
28.75
29
Time from MAY 1, [days]

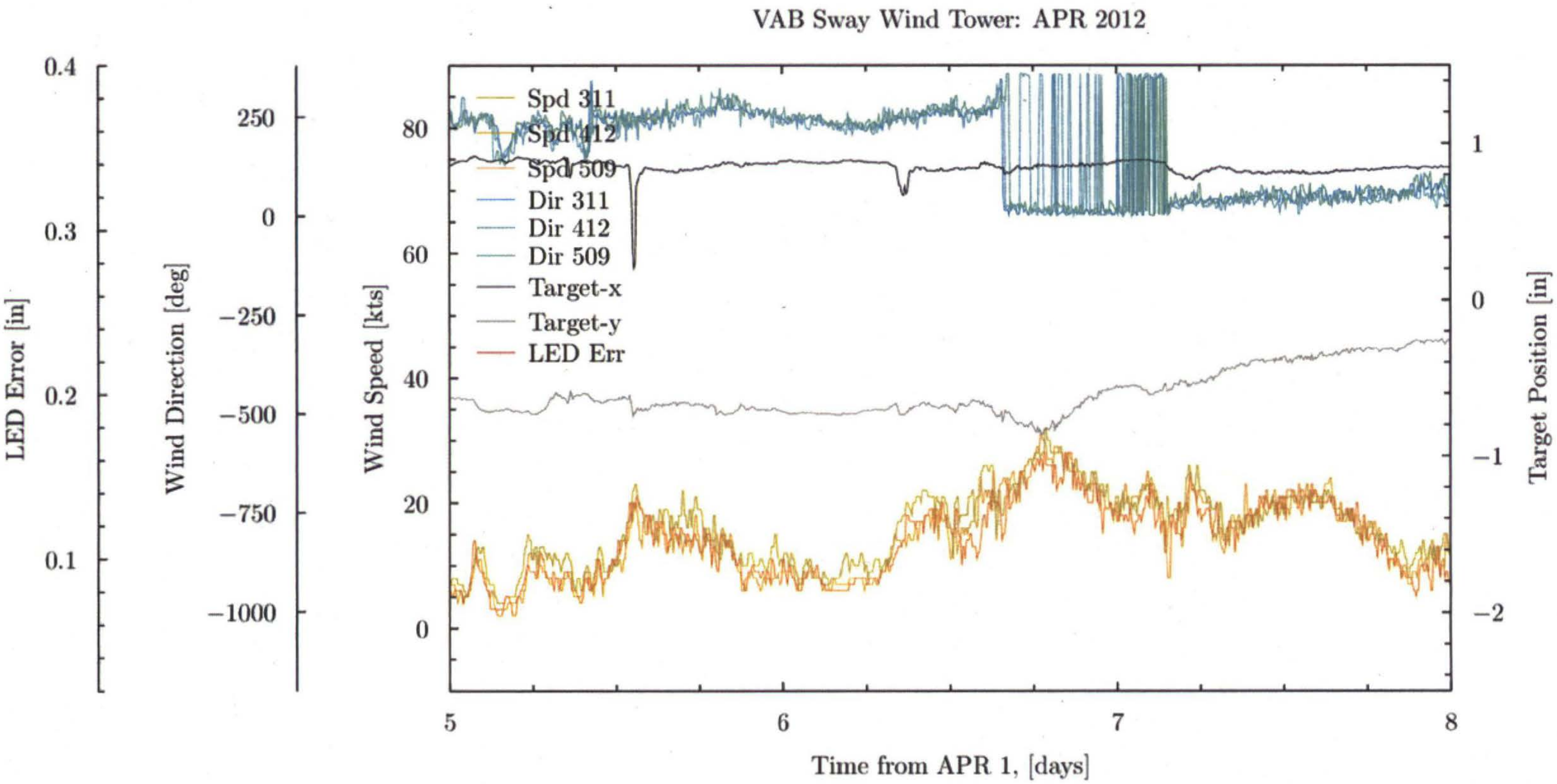
VAB Sway Wind Tower: APR 2012
Spd 311
Spd 412
Spd 509
Dir 311
Dir 412
Dir 509
Target-x
Target-y
LED Err
LED Error [in]
Wind Direction [deg]
Wind Speed [kts]
Target Position [in]
Time from APR 1, [days]
0.4
0.3
0.2
0.1
250
0
−250
−500
−750
−1000
80
60
40
20
0
1
0
−1
−2
5
6
7
8

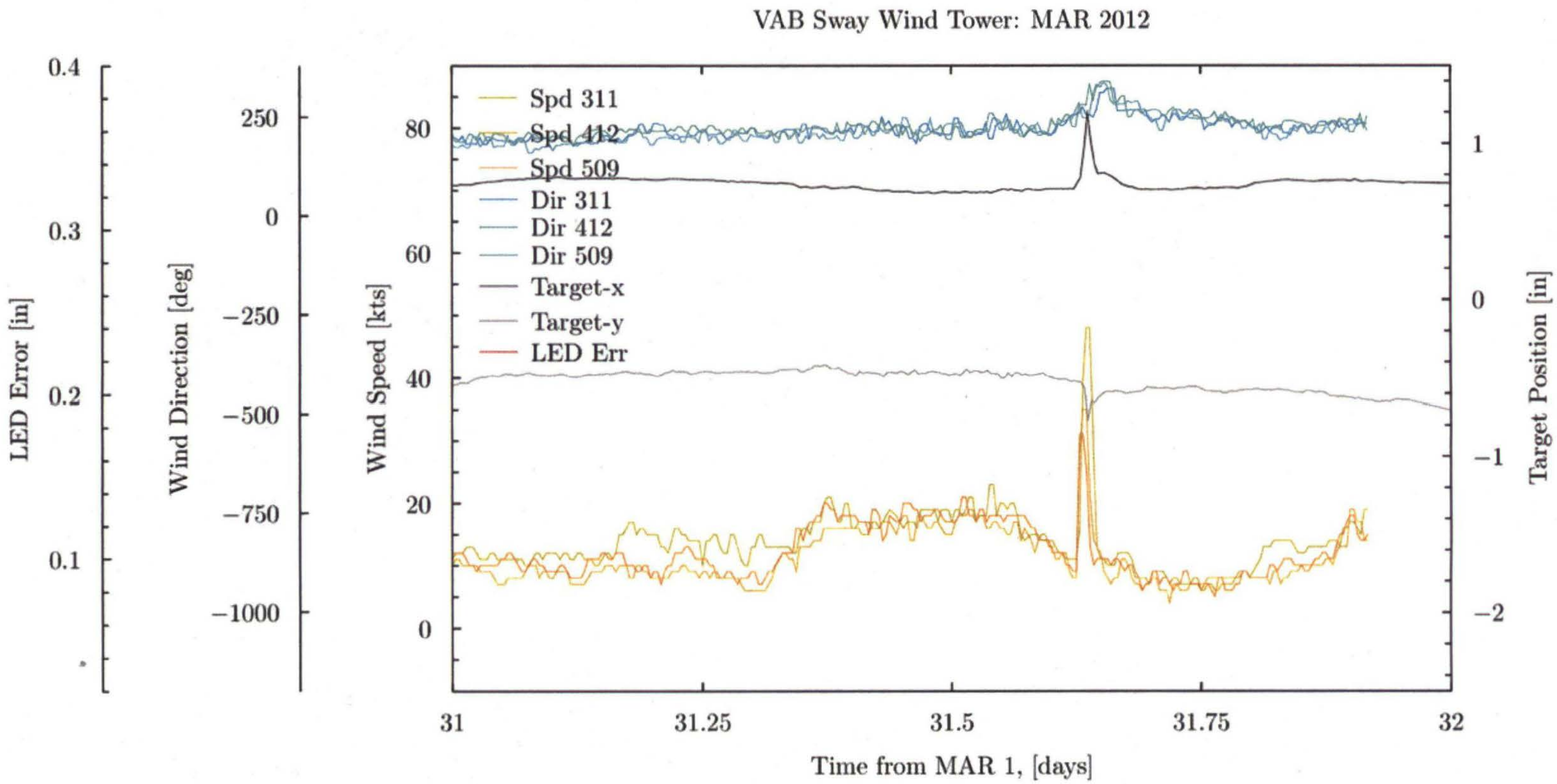
VAB Sway Wind Tower: MAR 2012
Spd 311
Spd 412
Spd 509
Dir 311
Dir 412
Dir 509
Target-x
Target-y
LED Err
LED Error [in]
Wind Direction [deg]
Wind Speed [kts]
Target Position [in]
Time from MAR 1, [days]
0.4
0.3
0.2
0.1
250
0
−250
−500
−750
−1000
80
60
40
20
0
1
0
−1
−2
31
31.25
31.5
31.75
32

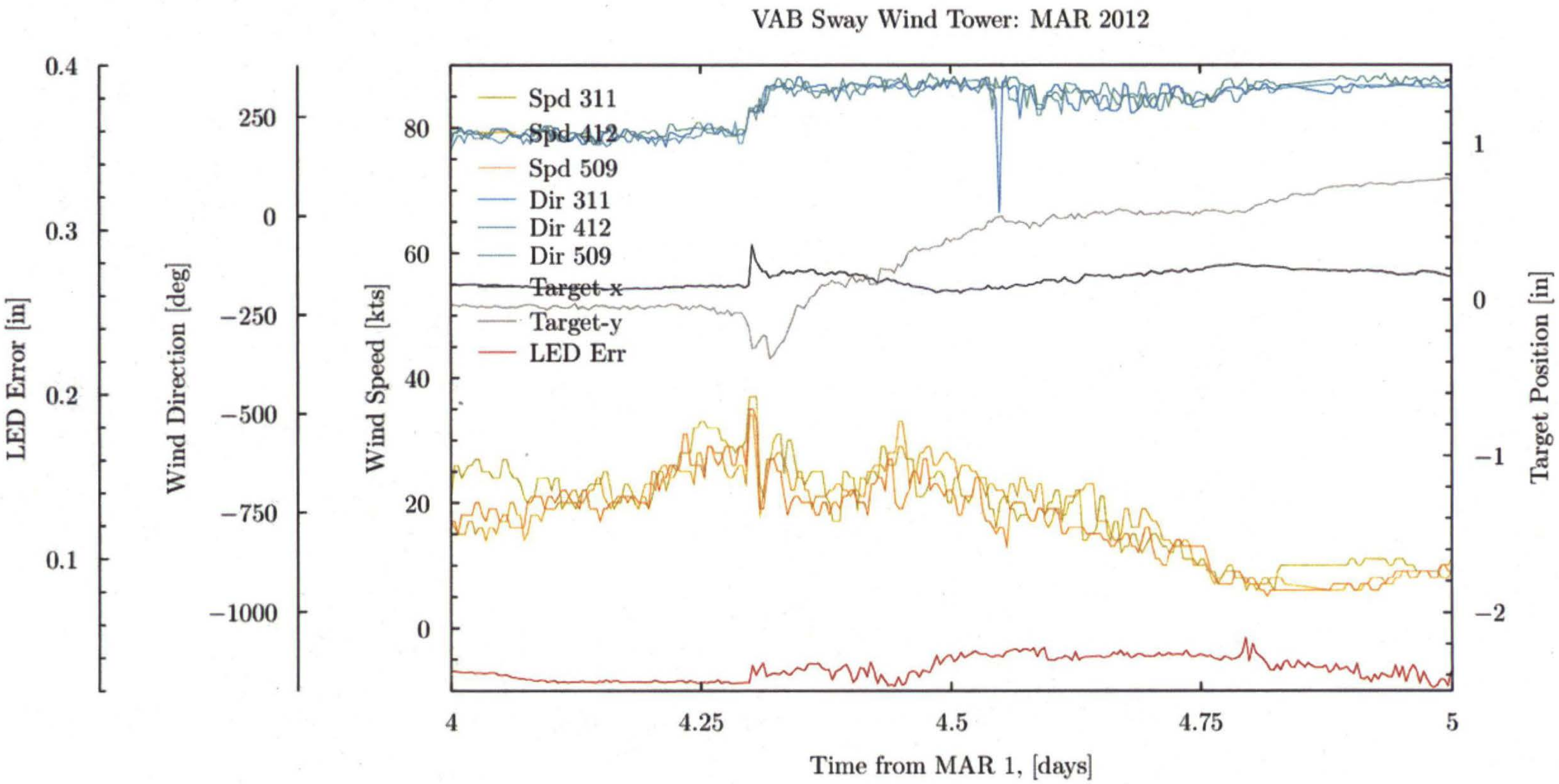
VAB Sway Wind Tower: MAR 2012
LED Error [in]
Wind Direction [deg]
Wind Speed [kts]
Target Position [in]
Time from MAR 1, [days]
Spd 311
Spd 412
Spd 509
Dir 311
Dir 412
Dir 509
Target-x
Target-y
LED Err
0.4
0.3
0.2
0.1
250
0
−250
−500
−750
−1000
80
60
40
20
0
1
0
−1
−2
4
4.25
4.5
4.75
5

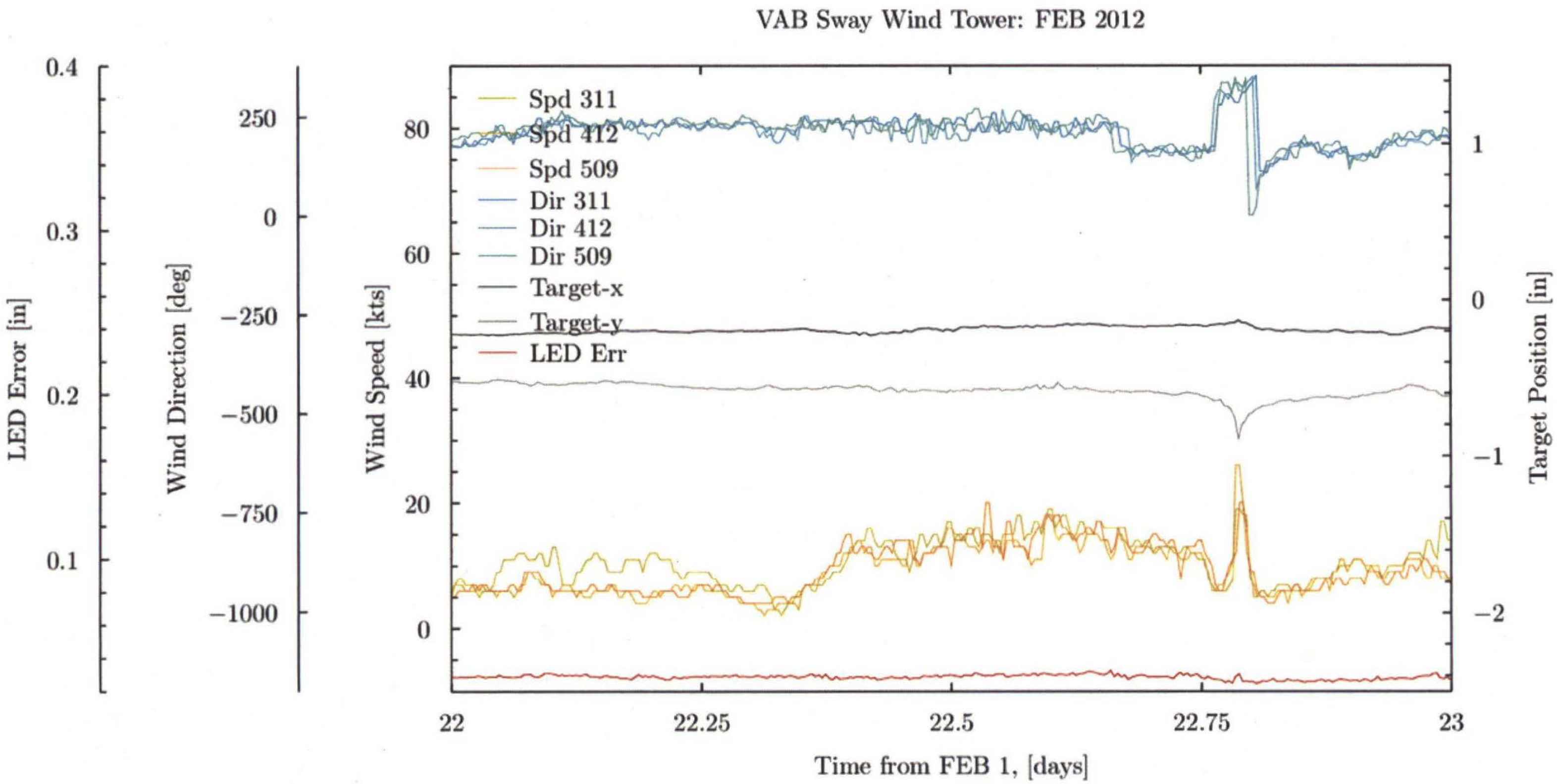
VAB Sway Wind Tower: FEB 2012
Spd 311
Spd 412
Spd 509
Dir 311
Dir 412
Dir 509
Target-x
Target-y
LED Err
LED Error [in]
0.4
0.3
0.2
0.1
Wind Direction [deg]
250
0
−250
−500
−750
−1000
Wind Speed [kts]
80
60
40
20
0
Target Position [in]
1
0
−1
−2
22
22.25
22.5
22.75
23
Time from FEB 1, [days]

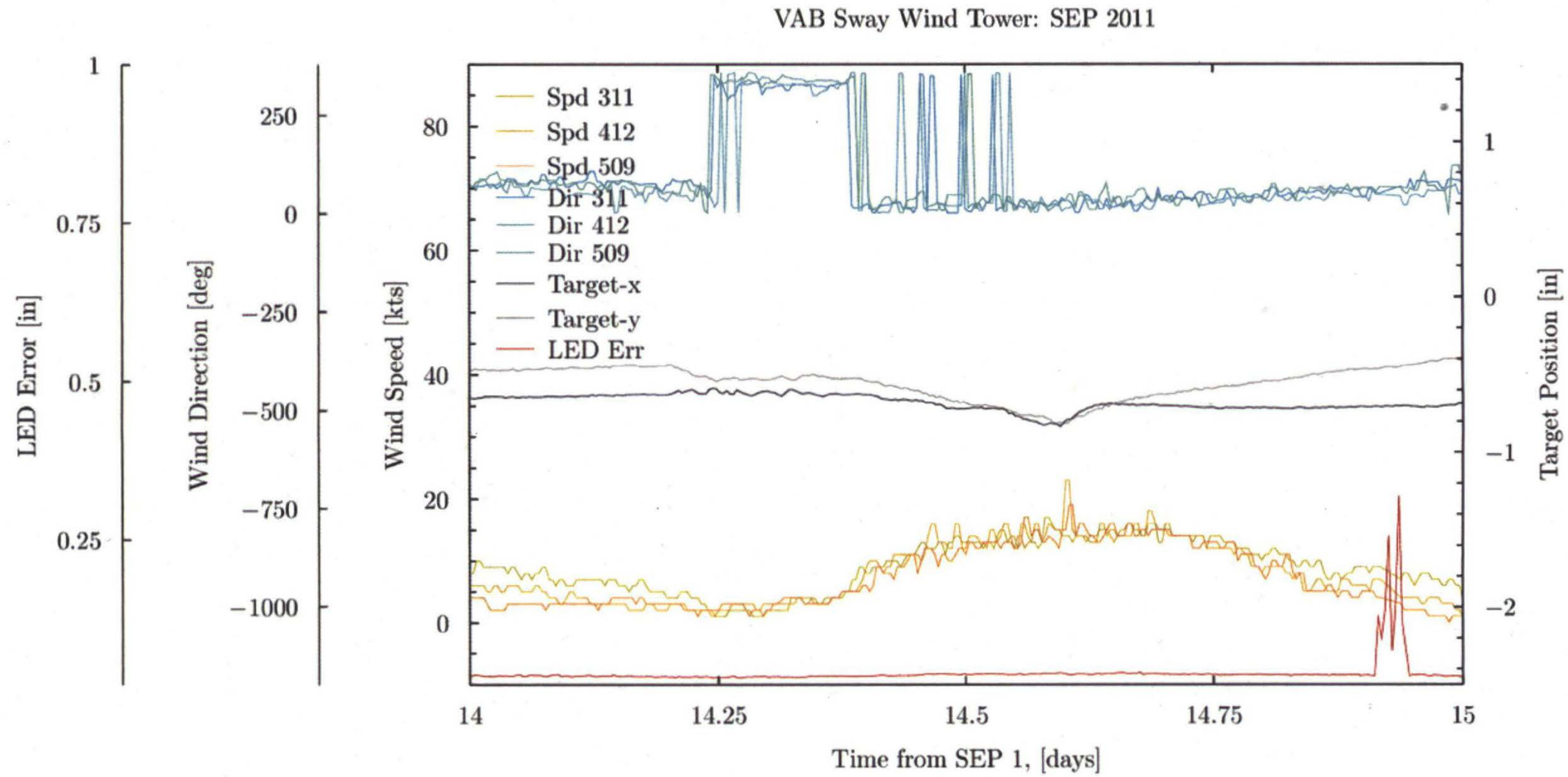
VAB Sway Wind Tower: SEP 2011
Spd 311
Spd 412
Spd 509
Dir 311
Dir 412
Dir 509
Target-x
Target-y
LED Err
LED Error [in]
Wind Direction [deg]
Wind Speed [kts]
Target Position [in]
Time from SEP 1, [days]
1
0.75
0.5
0.25
250
0
−250
−500
−750
−1000
80
60
40
20
0
1
0
−1
−2
14
14.25
14.5
14.75
15

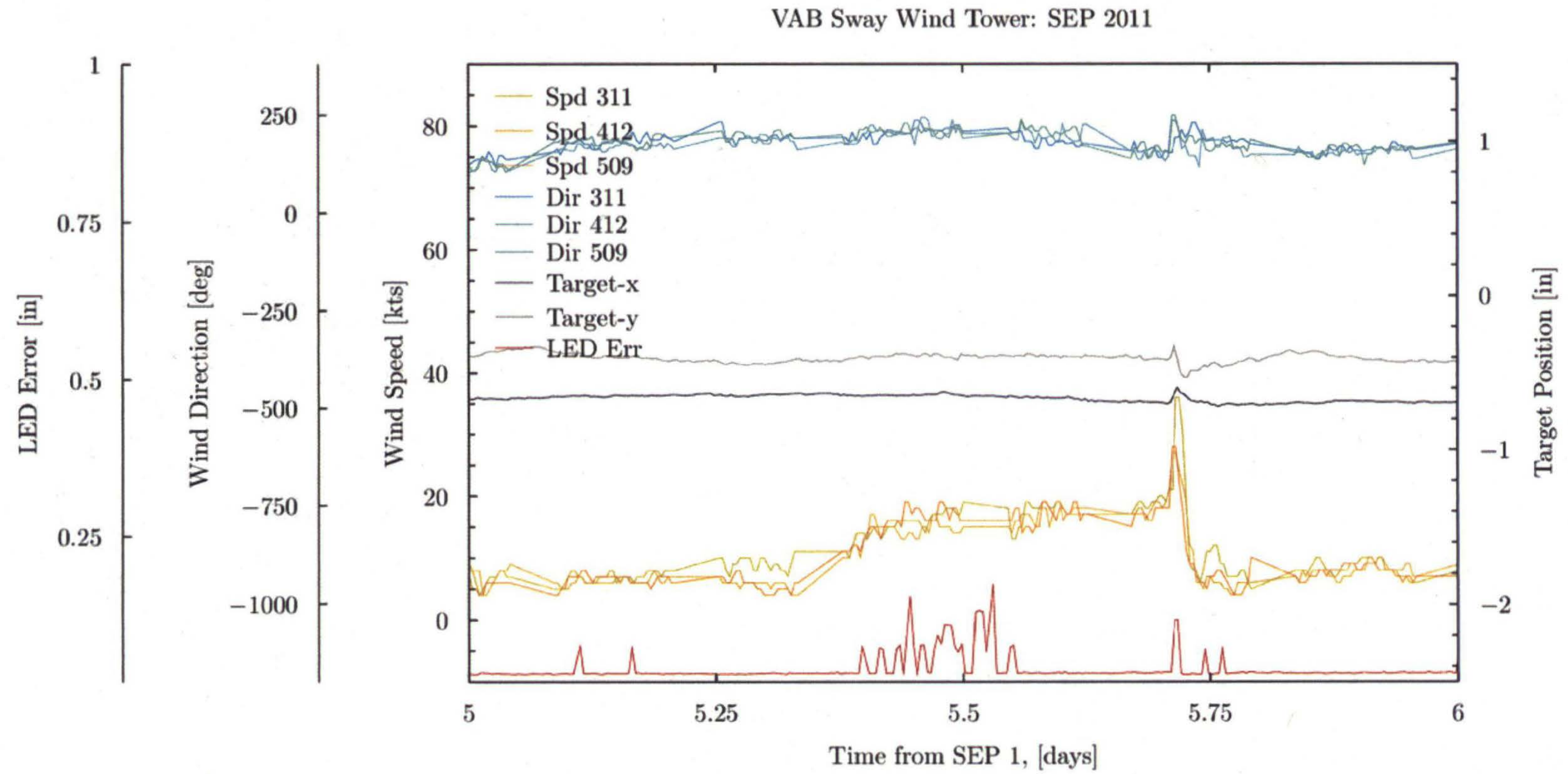
VAB Sway Wind Tower: SEP 2011
Spd 311
Spd 412
Spd 509
Dir 311
Dir 412
Dir 509
Target-x
Target-y
LED Err
LED Error [in]
Wind Direction [deg]
Wind Speed [kts]
Target Position [in]
Time from SEP 1, [days]
1
0.75
0.5
0.25
250
0
−250
−500
−750
−1000
80
60
40
20
0
1
0
−1
−2
5
5.25
5.5
5.75
6

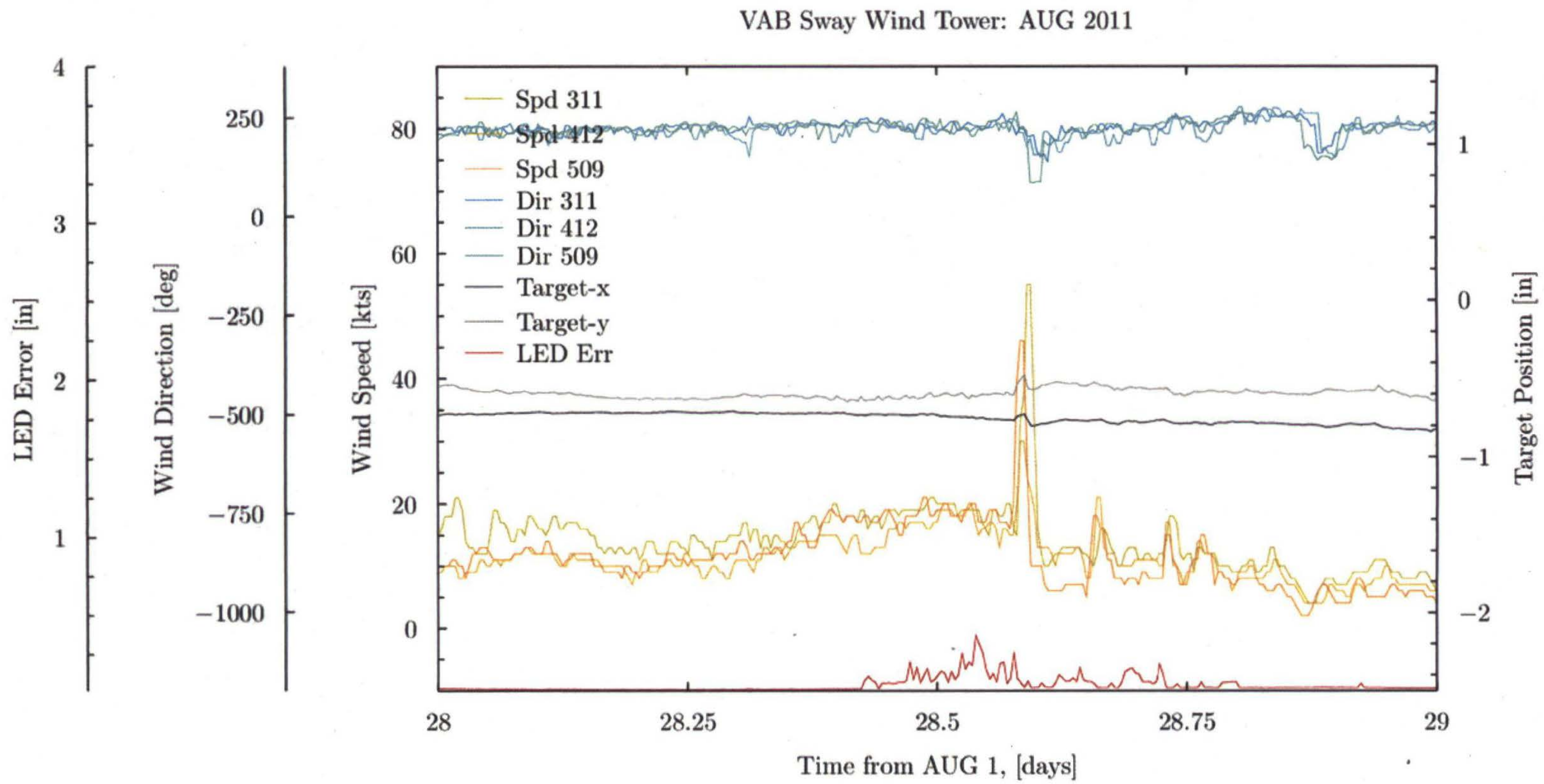

NASA/TM—2013–216320

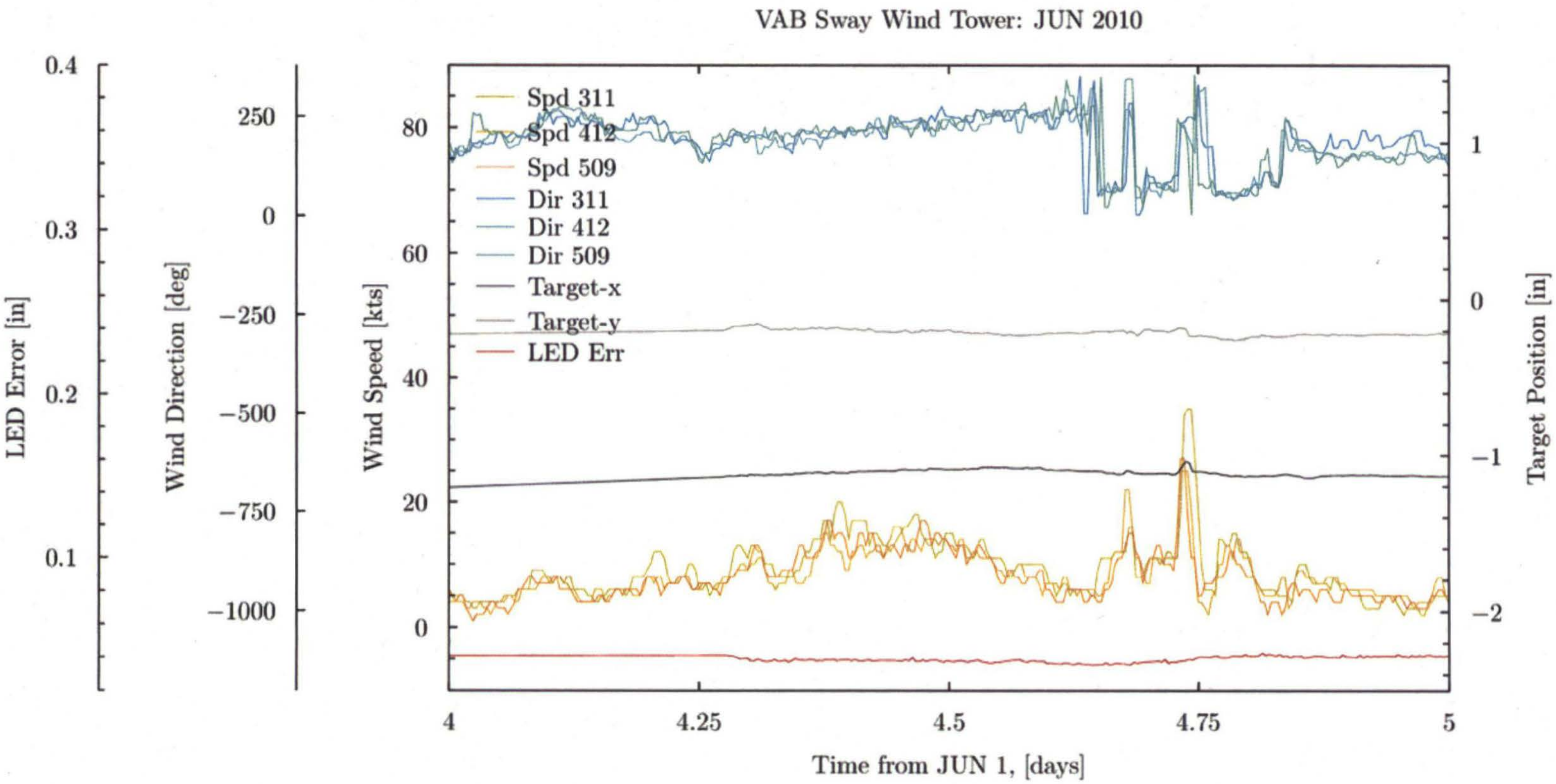
VAB Sway Wind Tower: JUN 2010
Spd 311
Spd 412
Spd 509
Dir 311
Dir 412
Dir 509
Target-x
Target-y
LED Err
LED Error [in]
0.4
0.3
0.2
0.1
Wind Direction [deg]
250
0
−250
−500
−750
−1000
Wind Speed [kts]
80
60
40
20
0
Target Position [in]
1
0
−1
−2
4
4.25
4.5
4.75
5
Time from JUN 1, [days]

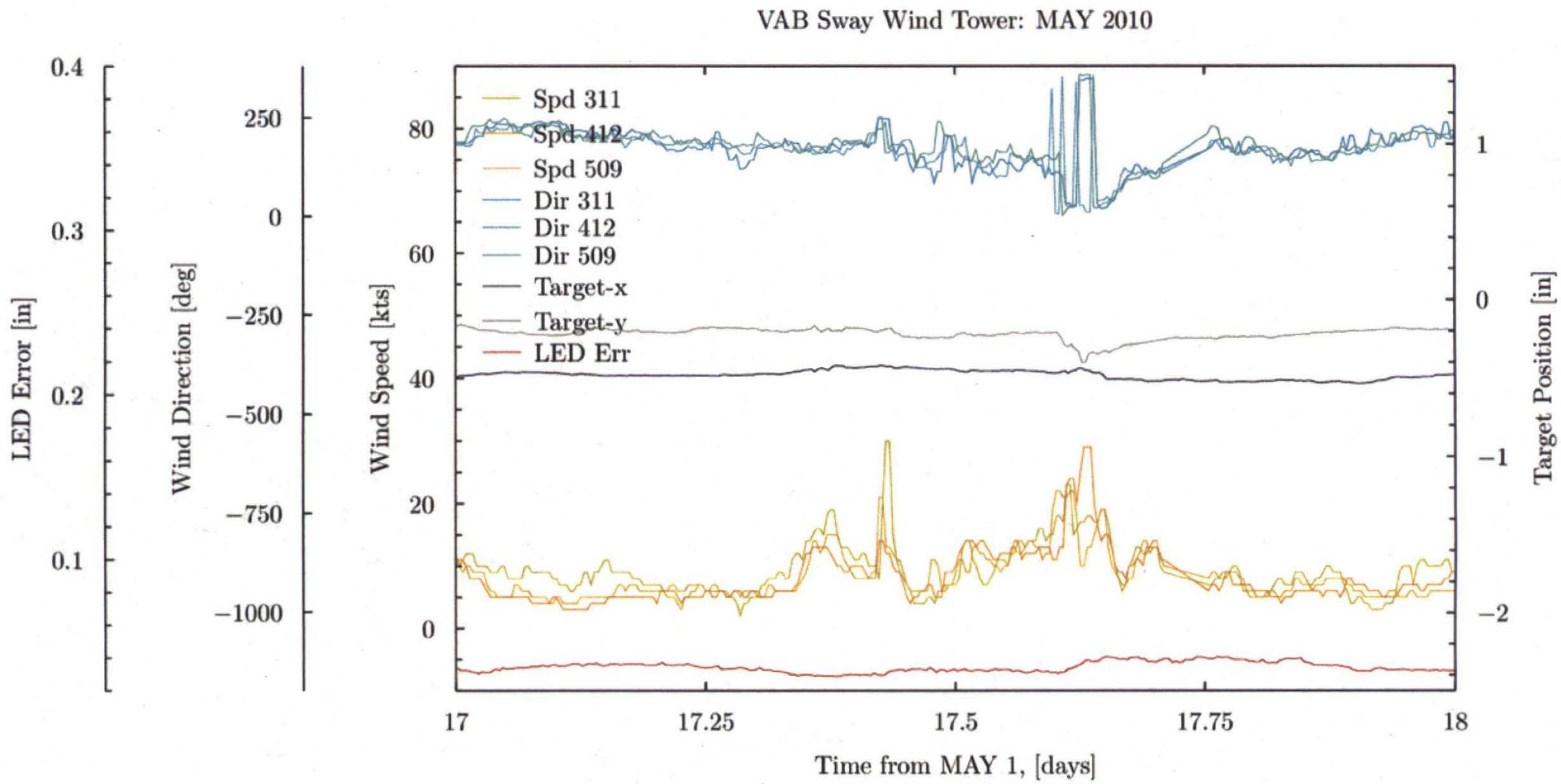

VAB Sway Wind Tower: MAY 2010
Spd 311
Spd 412
Spd 509
Dir 311
Dir 412
Dir 509
Target-x
Target-y
LED Err
LED Error [in]
Wind Direction [deg]
Wind Speed [kts]
Target Position [in]
Time from MAY 1, [days]
0.4
0.3
0.2
0.1
250
0
−250
−500
−750
−1000
80
60
40
20
0
1
0
−1
−2
17
17.25
17.5
17.75
18

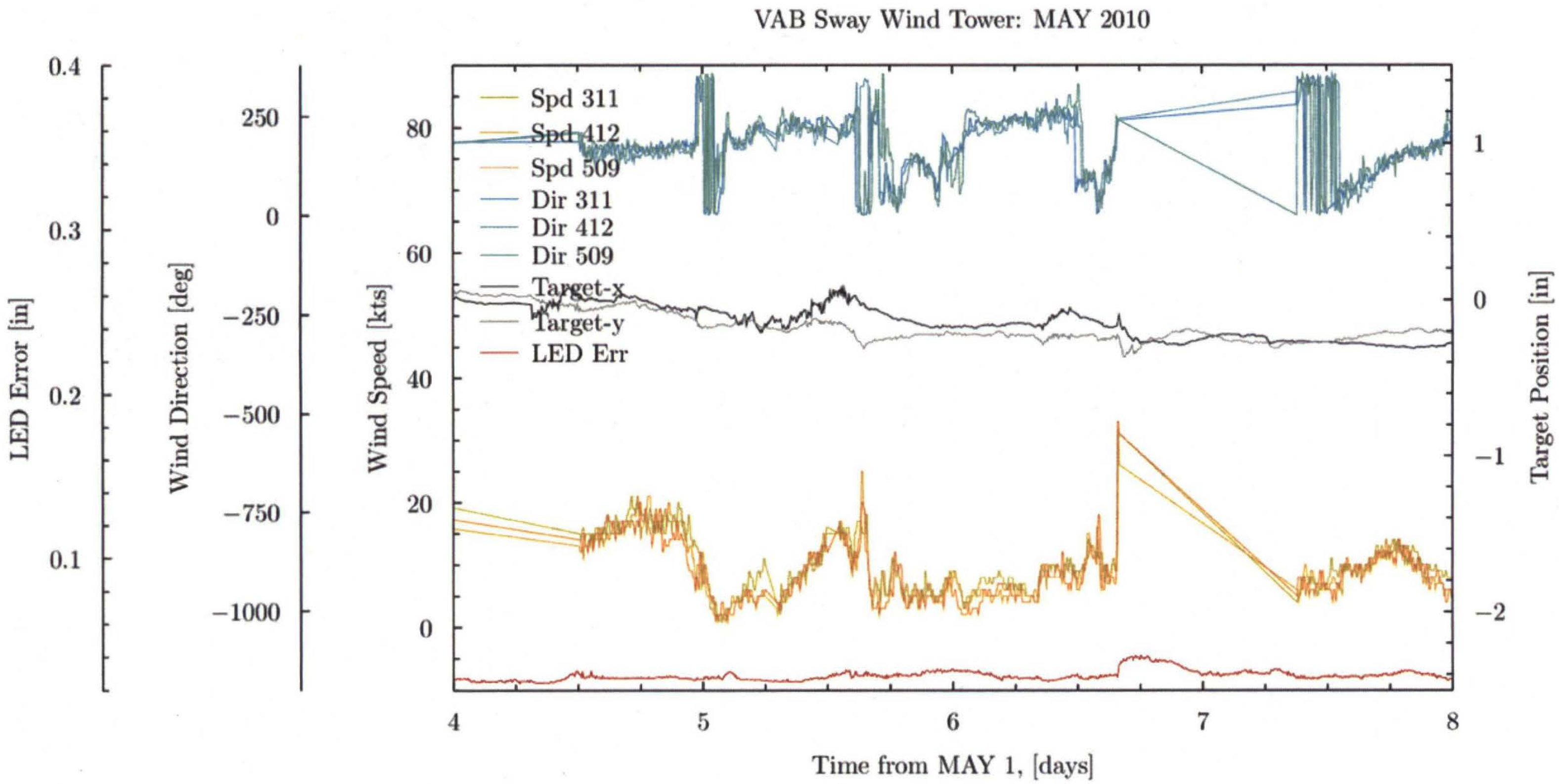
VAB Sway Wind Tower: MAY 2010
Spd 311
Spd 412
Spd 509
Dir 311
Dir 412
Dir 509
Target-x
Target-y
LED Err
LED Error [in]
Wind Direction [deg]
Wind Speed [kts]
Target Position [in]
Time from MAY 1, [days]
0.4
0.3
0.2
0.1
250
0
−250
−500
−750
−1000
80
60
40
20
0
1
0
−1
−2
4
5
6
7
8

APPENDIX B. DEVELOPMENT OF THE SWAY MATH MODEL

Development of Equation (1) begins with the following physical principles as starting points: the sway displacement of the building d is a quadratic function of the wind speed v and is separable from the quadratic dependence of the vertical height h of the sway measurement:

$$d(v,h) = f(v)g(h) \quad , \tag{B-1}$$

$$f(v) = \alpha v^2 \quad , \tag{B-2}$$

$$g(h) = \beta h^2 \quad , \tag{B-3}$$

where α is parameter dependent on the building structure. The parameter β is equal to L^{-2} where L is the building height.

The data from Table 2 is plotted in Figure B-1, along with Equation (B-1) with $g(L) = 1$. The parameter α is chosen to fit the data. The key to the strategy leading to the sway model represented by Equation (1) is finding the standard deviation of the data, corresponding to Table 2.

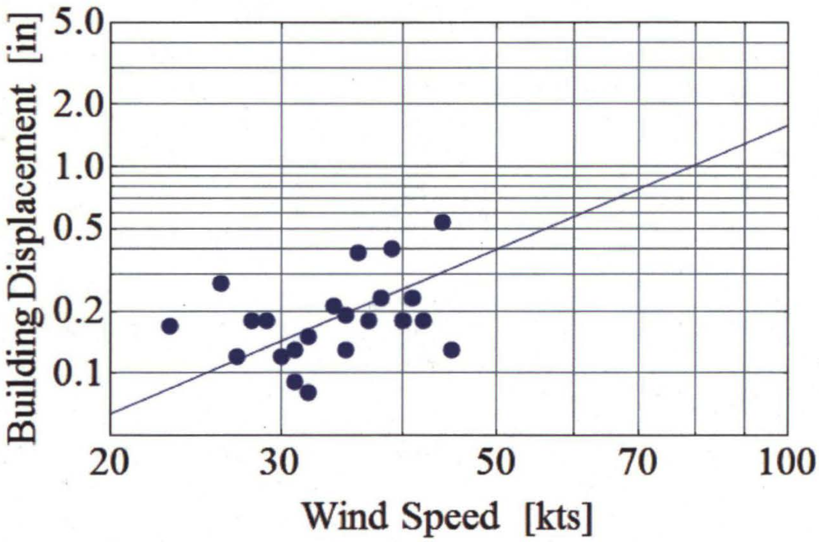

Figure B-1. The data from Table 2 with Equation (B-1) with $g(L) = 1$.

The first step is to rotate the coordinate system so that the mean of the data equals zero. The following variable substitution will simplify this procedure (where "log" is base 10):

$$u = \log d - u_0 \quad , \tag{B-4}$$

$$w = \log v \quad , \tag{B-5}$$

where $u_0 \equiv \log\alpha$.

Figure B-2 shows Table 2 data plotted using the transformed variables (u w). Note that both plots are practically identical, where only the axis labeling and plot range has changed, as well as vertical offset, u_0.

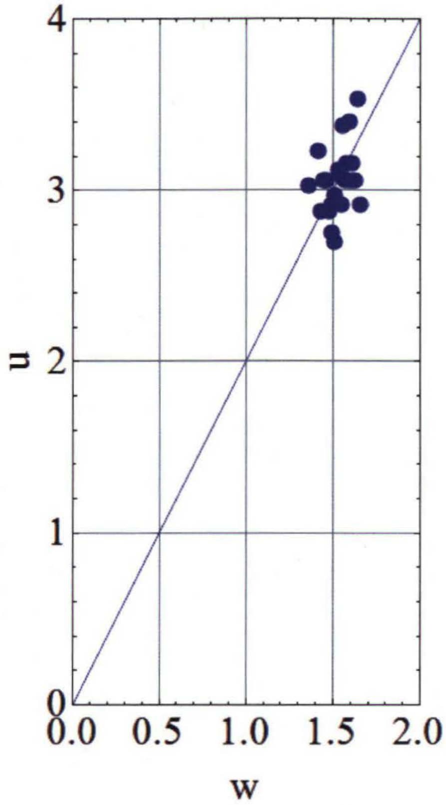

Figure B-2. Data from Table 2 plotted using variable transformations, Equations (B-4) and (B-5). The solid line has a slope of 2 and is just $u(w) = 2w$.

The vector formed by (w u) is now rotated by an angle $\theta = \tan^{-1} 2$, which has the effect of forcing the slope of the fit in Figure B-1 to zero:

$$\begin{pmatrix} w' \\ u' \end{pmatrix} = \begin{pmatrix} \cos\theta & \sin\theta \\ -\sin\theta & \cos\theta \end{pmatrix} \cdot \begin{pmatrix} w \\ u \end{pmatrix} \quad . \tag{B-6}$$

Figure B-3 is Table 2 data after application of Equation (B-6).

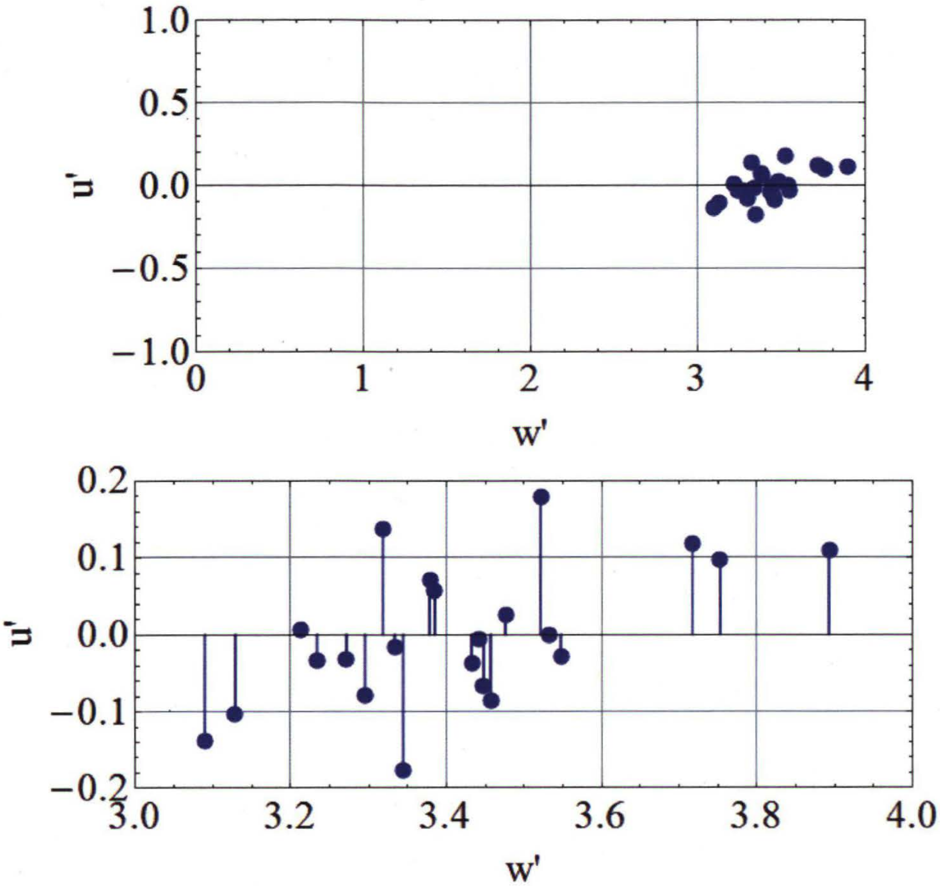

Figure B-3. Data from Figure B-2 plotted after undergoing the rotation transformation of Equation (B-6). The bottom plot is a zoomed-in version of the top plot. The line fit from the previous plot, $u(w) = 2w$, is now $u'(w') = 0$.

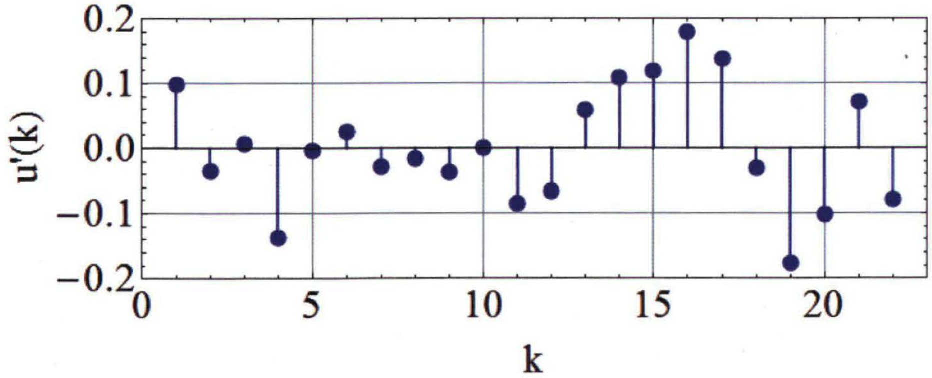

Figure B-4. The u'_k sequence from Figure B-3 with same ordering shown in Table 2.

The next step is to compute the mean and standard deviation of the data in Figure B-3. Before doing so, it is helpful to replot Figure B-3 as a sequence of data u'_k , dropping the w'_k, since the random variable of interest is u'_k. Figure B-4 is the u'_k sequence from Figure B-3, in ascending order, the same ordering shown in Table 2.

Now it is a simple matter to calculate the mean μ and standard deviation σ of the sequence of N data points shown in Figure B-4:

$$\mu = \sum_{k=1}^{N} u'_k \quad , \tag{B-7}$$

$$\sigma = \left(\frac{1}{N-1} \sum_{k=1}^{N} (\mu - u'_k)^2 \right)^{1/2} \quad . \tag{B-8}$$

The mean must equal zero, and it is necessary to iteratively adjust α , where $u_0 \equiv \log\alpha$, so that $\mu \to 0$. The result is shown in Table B-1.

Table B-1. Adjusted data plotted in Figure B-4, with $\alpha = 0.0001591$.

k	u'_k
1	0.0976349
2	−0.0342895
3	0.0066372
4	−0.13811
5	−0.0049171
6	0.0257814
7	−0.0292712
8	−0.0160197
9	−0.037004
10	0.000245142
11	−0.08624
12	−0.0672877
13	0.0576297
14	0.109065
15	0.118765
16	0.178798
17	0.13657
18	−0.0314805
19	−0.176244
20	−0.102901
21	0.0712608
22	−0.0786225
μ	-1.905×10^{-10}
σ	0.0922

Table B-1 and Figure B-4 depict a transformed coordinate system where the sway measurement "noise" is independent of wind speed and only dependent on the errors resulting from random unknowns such as the wind correction factor between wind tower height and VAB height. Figure B-3 hints that as the horizontal variable w' increases, the running average mean may not be zero. However, without higher wind speed measurements than what was observed during the period of this investigation, it is not constructive to infer a wind speed dependence in Figure B-3. But this could be worth reinvestigating for future analysis refinement.

To get back to the original coordinate system where building displacement is a function of wind velocity, all of the previous transformations must be reversed. The first step on the way back is to express the function in Figure B-4 as a vector composed of a random variable x with zero mean, and a value above the mean given by $n\sigma$. This vector is then acted upon by a rotation matrix that is the inverse of the original rotation:

$$\begin{pmatrix} w'' \\ u'' \end{pmatrix} = \begin{pmatrix} \cos\theta & -\sin\theta \\ \sin\theta & \cos\theta \end{pmatrix} \cdot \begin{pmatrix} x \\ n\sigma \end{pmatrix}$$

$$= \begin{pmatrix} x\cos\theta - n\sigma\sin\theta \\ n\sigma\cos\theta + x\sin\theta \end{pmatrix} \quad . \tag{B-9}$$

The two components can be combined, eliminating x :

$$u'' = n\sigma\cos\theta + w''\tan\theta \quad . \tag{B-10}$$

The last step is to add u_0 and take the anti-log (and dropping the double primes):

$$\begin{aligned} d(n,v) &= 10^{n\sigma/\cos\theta + w\tan\theta + u_0} \\ &= 10^{n\sigma\sec\theta + \log v\tan\theta + \log\alpha} \\ &= \alpha\ 10^{n\sigma\sqrt{5}}v^2 \\ &= \alpha\ e^{bn\sigma}v^2 \quad . \end{aligned} \tag{B-11}$$

Equation (B-11) is now Equation (B-2). Note that $b \equiv \sqrt{5}\ \ln 10$, since $\sec\theta = \sec\left(\tan^{-1}2\right) = \sqrt{5}$. Including the height dependence, Equation (B-3):

$$d(n,v,h) = \alpha\ e^{bn\sigma}v^2\left(\frac{h}{L}\right)^2 \quad , \tag{B-12}$$

yields the desired result, Equation (1).